

FRONT MATTER

Title:

Energetic demands of extreme temperatures reduce cryptobenthic coral reef fish diversity and functioning

Authors:

Simon J. Brandl^{1,2,3,4*†}, Jacob L. Johansen^{5,6†}, Jordan M. Casey^{3,4}, Luke Tornabene⁷, Renato A. Morais^{8,9}, John A. Burt⁶

Affiliations:

¹ Department of Biological Sciences, Simon Fraser University, Burnaby, BC, Canada

² CESAB - FRB, 5 Rue de l'École de Médecine, 34000, Montpellier, France

³ PSL Université Paris: CNRS-EPHE-UPVD USR3278 CRILOBE, Université de Perpignan, Perpignan, France

⁴ Laboratoire d'Excellence "CORAIL," Perpignan, France

⁵ Hawai'i Institute of Marine Biology, University of Hawai'i at Manoa, Kane'ohe, HI, USA

⁶ Marine Biology Laboratory, Centre for Genomics and Systems Biology, New York University Abu Dhabi, Abu Dhabi, United Arab Emirates

⁷ School of Aquatic and Fishery Sciences and the Burke Museum of Natural History and Culture, University of Washington, Seattle, WA, USA

⁸ ARC Centre of Excellence for Coral Reef Studies, James Cook University, Townsville, QLD, Australia

⁹ College of Science and Engineering, James Cook University, Townsville, QLD, Australia

† indicates shared first authorship

Abstract:

Cascading effects of organismal tolerances to global change on community assembly and functioning are poorly understood. Here, we show that cryptobenthic fishes on the world's hottest coral reefs (southeastern Arabian Gulf) are dramatically less diverse and abundant than in the thermally benign Gulf of Oman, despite no difference in live coral cover. This is not driven by organismal temperature tolerances. Rather, impoverished body conditions of Arabian Gulf populations highlight increased energetic costs of growth and homeostasis at higher temperatures, while intraspecific dietary differences suggest that these costs need to be met with a distinct, narrower set of resources. By creating an energetic double jeopardy, conditions in the southeastern Arabian Gulf, which mirror forecasted end-of-century water temperatures, prohibit the persistence of many small-bodied species and reduce the production, transfer, and replenishment of cryptobenthic fish biomass. Future reefs may thus lose a critical element of their fast-paced dynamics, independent of coral loss.

43 **MAIN TEXT**

44
45 **The manuscript should be a maximum of 15,000 words.**

46
47 **Introduction**

48 Why do some species occur in a given location while similar taxa are missing? And how
49 do resulting species assemblages affect rates of ecological processes? As escalating human
50 impacts on the biosphere deplete and re-shuffle biological communities across ecosystems (1, 2),
51 answers to these questions are key to our quest to preserve biodiversity and ecosystem services to
52 humanity (3, 4).

53 A species' presence at a given location is mediated by a hierarchical interplay between
54 organismal traits (e.g., temperature tolerance, trophic niche), environmental conditions (e.g.,
55 temperature, salinity), biogeographic history, and stochastic events (e.g., extinction, dispersal,
56 lottery dynamics) (5–8). Furthermore, the identity and diversity of species affect rates of
57 ecosystem functioning, including processes that are critical to human well-being, such as primary
58 or consumer productivity (9–11). However, by modifying abiotic conditions, species' niches, and
59 biotic interactions, global stressors such as climate change can interfere with these dynamics
60 through numerous pathways (12–14). At the organismal level, changes in environmental factors,
61 particularly temperature, affect internal physiological processes (15), which, if not lethal, will
62 alter organismal energy expenditure (16–18). Changes in organismal energy budgets subsequently
63 drive resource acquisition (e.g. feeding rates, prey species) and how resulting energy is allocated
64 to life-supporting processes (homeostasis), growth, and reproduction (19–22). Dynamics of
65 energy acquisition and investment, which are often investigated through the lens of ecological
66 niche and fitness, are the basis of modern coexistence theory and critical for our understanding of
67 community assembly dynamics (23) and the rate of ecological processes that underpin energy and
68 nutrient fluxes through ecosystems (24). Integration across levels of biological organization is,
69 therefore, crucial to understand the effects of global environmental change on our planet's
70 ecosystems (25).

71 Coral reefs are the most diverse marine ecosystem, and their productivity provides vital services
72 for more than 500 million people worldwide (26). Scleractinian corals, the foundation species of
73 tropical reefs, show high thermal sensitivity that has led to the rapid global decline of coral reef
74 ecosystems (27). In wake of losing coral habitat, communities of the most prominent reef
75 consumers, teleost fishes, can decline or shift in composition (28–31), which directly affects the
76 provision of resources to people dependent on reef fisheries (32). Nevertheless, recent evidence
77 suggests that many fish species will be able to cope with (or even benefit from) live coral loss, at
78 least in the short-term (32–34). However, tropical marine ectotherms are typically adapted to a
79 relatively narrow thermal environment, so reef fishes may also be vulnerable to the direct effects
80 of changing water temperatures (16, 35, 36). Consequently, the direct responses of reef fishes to
81 climate change and their potential to adapt to different thermal regimes might be as important as
82 indirect, habitat-mediated responses (37–39).

83 Despite marked differences in species-specific tolerances to higher temperatures (40–44), most
84 reef fish species suffer from non-lethal (45) adverse physiological, developmental, or behavioral
85 responses when exposed to temperatures outside of their normal range. Current understanding
86 suggests long-term deleterious effects on reef fish populations in the wild (37), but few cases of
87 direct temperature-mediated population declines have been documented for *in situ* reef fish
88 communities (46). One factor that ameliorates the adverse effects of rising temperatures in the
89 wild may be transgenerational acclimation and adaptation, which can enhance the performance of
90 offspring in higher temperatures through developmental, genetic, or epigenetic pathways (39, 47).
91 Transgenerational adaptation has been shown in a few model species (39, 47, 48), but demands

increased energetic investments (47, 49). It is presently unresolved whether this process can truly enhance the survival of reef fishes in competitive, uncontrolled environments and how species-specific temperature tolerance differences may mediate coexistence in ecological communities.

Cryptobenthic fishes are the smallest of all reef fishes, rarely exceeding 50mm in maximum body size (50). They account for almost half of all reef fish species and are numerically abundant and ubiquitous on reefs worldwide (50–53). Due to their small body size, these fishes have evolved a unique life history strategy of rapid growth, high mortality, and continuous larval replenishment, and they may play an important role in coral reef trophodynamics (54). Their small body size and associated life-history also promise exceptional traceability concerning the effects of, and responses to, increasing temperatures (50). Limited gill surface area, unfavorable mass to surface ratios, high mass-specific metabolism, and other physiological challenges resulting from their minute size suggest that cryptobenthics are particularly susceptible to temperature fluctuations (42, 50, 55). Due to their limited mobility and close association with the benthos (56), mitigation of temperature extremes through migration is often not viable, and notable community composition shifts following changes in the benthic community structure have been detected (31, 57). However, their extremely high generational turnover (7.4 generations per year in some species (54, 58)) and prevalence of benthic clutch spawning and parental care (50) may make them ideally suited for transgenerational adaptation to changing conditions (37). In fact, an extremely fast evolutionary clock has been implicated as a driver for rapid speciation in cryptobenthic fishes (59), which may permit similarly fast microevolutionary changes (i.e., rapid adaption). Thus, cryptobenthic fishes may be well-suited to detect the impact of environmental change on organisms and populations, with promising insights into whether transgenerational plasticity or adaptation can provide pathways to the persistence of coral reef fishes in warming oceans.

Here, we quantify cryptobenthic community structure, species- and population-specific physiological and dietary traits, and contributions to ecosystem functioning in the world's hottest coral reef environment, the southeastern Arabian Gulf, and we compare the resulting patterns with the spatially proximate, but more environmentally benign, Gulf of Oman. Specifically, the goal of our study was to 1) describe cryptobenthic fish assemblages across the two locations, 2) identify organismal traits that permit or preclude existence in the Arabian Gulf, and 3) determine the consequences of these results for the production, provision, and renewal of cryptobenthic fish biomass (25).

Results

Reefs in the shallow southern Arabian Gulf can range from 16° C in the winter months to over 36° C in the summer, while reefs in the nearby Gulf of Oman fluctuate within a much narrower temperature range (approximately 22° C to 32° C) (60). Maximum temperatures on reefs along the Arabian Gulf coast of the United Arab Emirates mirror forecasted temperatures for most tropical coral reefs in the end of the century (61). Despite the seemingly unfavorable conditions for tropical reef building corals, corals have persisted in this region for approximately 15,000 years, with the modern coastline harboring coral reef structures for circa 6,000 years (61). Therefore, the Arabian Gulf represents an exceptional natural laboratory to examine the capacity of reef organisms to cope with unfavorable conditions and how this influences the diversity and dynamics that underpin modern coral reefs (Fig. 1a,b).

Cryptobenthic reef fish assemblages markedly differed between the Arabian Gulf and the Gulf of Oman. Reefs in the Gulf of Oman harbored a higher diversity (Bayesian hierarchical model estimate: *Gulf of Oman*: $\beta = 0.73$ [0.44, 1.01; lower and upper 95% credible interval]) and density (*Gulf of Oman*: $\beta = 1.77$ [1.03, 2.58]) of cryptobenthic fishes (Fig. 1a,b), but standing biomass estimates were comparable (*Gulf of Oman*: $\beta = 0.63$ [-0.54, 1.71]; Fig. 1c). Similarly, the composition of cryptobenthic communities greatly varied between the two locations (Fig. 2a), with no overlap among convex hull polygons in the non-metric multidimensional scaling (nMDS) ordination and a strong effect of *Location* in the PERMANOVA using a site-by-species dissimilarity matrix (*Location*: $df = 1$, $F = 13.58$, $P = 0.001$, $R^2 = 0.46$). There were 29 unique species in the Gulf of Oman, 13 unique species in the Arabian Gulf, and 16 species shared among the two locations. Importantly, of the 29 unique Gulf of Oman species, 89.7% have records from the northern Arabian Gulf in Kuwait and Saudi Arabia (but not the southeastern region), where summer conditions are much less extreme (62) (Fig 1; Table S1). In contrast to the cryptobenthic fish community, there were no differences in coral cover (Bayesian hierarchical model: *Gulf of Oman*: $\beta = 0.02$ [-1.30, 1.42]) nor overall benthic community structure as revealed by a PERMANOVA (*Location*: $df = 1$, $F = 1.63$, $P = 0.187$, $R^2 = 0.09$; Fig. 2b). Thus, despite broadly comparable benthic conditions, including similar live coral cover, cryptobenthic fish assemblages strongly differed between the two locations.

We then tested whether organismal temperature tolerance can explain the absence of species from the thermally extreme southeastern Arabian Gulf, despite their recorded presence in more benign parts of the Arabian Gulf. Notwithstanding distinct thermal regimes at the two locations and the drastic differences in cryptobenthic fish assemblages, species-specific critical thermal tolerance limits did not explain the absence of three common Gulf of Oman species in the Arabian Gulf (Fig. 3). The mean critical thermal maximum tolerance limits (ct_{max}) of all species, regardless of origin, equaled or surpassed the maximum summer temperatures typically recorded in the Arabian Gulf (36.0 °C). *Helcogramma fuscopinna* (a Gulf of Oman species) had the lowest heat tolerance at 36.0 ± 0.11 °C, while *Coryogalops anomolus* from the Arabian Gulf had the greatest heat tolerance (38.4 ± 0.06 °C). While there were no population differences in heat tolerance for *Enneapterygius ventermaculus* (possibly due to limited samples from the Gulf of Oman), the Arabian Gulf population of *Ecsenius pulcher* showed considerably greater heat tolerance than their Gulf of Oman counterparts, providing evidence for enhanced thermal tolerance in this

species. Despite considerable interspecific differences and evidence for intraspecific thermal plasticity (Table S2), mean predicted maximum posterior heat tolerances of all species restricted to the Gulf of Oman were within the 95% bounds of the species present in the Arabian Gulf.

In terms of critical thermal minima (ct_{min}), all species, regardless of origin, tolerated the minimum winter temperature of the UAE Arabian Gulf at 16 °C. Among individuals sampled from the Gulf of Oman population, *E. pulcher* had the greatest tolerance to cold ($ct_{min} = 11.3 \pm 0.1$ °C), while *E. ventermaculus* had the poorest tolerance (13.3 ± 0.1 °C). The cold-tolerance of *E. ventermaculus* in the Arabian Gulf substantially exceeded its Gulf of Oman counterpart (Table S3), which provides evidence from a second population for intraspecific plasticity in thermal tolerances across the two locations. Although there were again species-specific differences in the critical thermal minimum, mean cold tolerances of all Gulf of Oman species also fell within the 95% credible bounds of the species present in the Arabian Gulf (Fig. 3a).

To further examine potential drivers of cryptobenthic community structure, we quantified species' diets in the two locations using gut content DNA metabarcoding (63) across 88 individuals belonging to six species (*C. anomolus*, *E. pulcher*, and *E. ventermaculus* [Arabian Gulf and Gulf of Oman populations]; *Antennablennius adenensis*, *Eviota guttata*, and *Heteroleotris vulgaris* [Gulf of Oman only]). We targeted the cytochrome *c* oxidase subunit I (COI) gene region with primers that preferentially amplify metazoans and the 23S rRNA gene region with primers designed to amplify algae. Across all examined fishes, COI metabarcoding yielded a total of 547 unique operational taxonomic units (OTUs), while 23S metabarcoding yielded 3,009 unique exact sequence variants (ESVs). Bipartite dietary network trees and modularity analyses for the COI marker showed strong separations between the Arabian Gulf and Gulf of Oman populations (Fig. 4). The COI network contained five distinct modules (modularity = 0.472), with 92.3% of individuals from the Arabian Gulf distributed across two modules. Module V contained seven out of ten individuals of *C. anomolus* from the Arabian Gulf, 8 out of 9 individuals of *E. ventermaculus* from the Arabian Gulf, and one *E. guttata* from the Gulf of Oman. The remaining individuals of *C. anomolus* and *E. ventermaculus* from the Arabian Gulf clustered with *E. pulcher* from the Arabian Gulf (five out of seven), four Gulf of Oman individuals of *C. anomolus*, and a single *H. vulgaris* in module II (Fig. 4a,b). The 23S marker also revealed five modules (modularity = 0.359) but showed an even stronger regional separation. All individuals from the Arabian Gulf (except for one *C. anomolus*) were united in a single module (module III), which contained no Gulf of Oman individuals (Fig. 4c,d). While some species separated into distinct modules, location specific differences superseded taxonomic boundaries. With the exception of *C. anomolus*, species occurring in both locations showed strong dietary differences, while broadly overlapping with other species in the Gulf of Oman.

Prey diversity rarefaction curves in the Gulf of Oman showed that *E. pulcher*, a purportedly herbivorous species(64), ingested the widest variety of animal prey species (COI marker), followed by *E. ventermaculus* (Fig. S1). For both species, Gulf of Oman populations consumed a higher diversity of prey items than Arabian Gulf populations. Only *C. anomolus* showed no clear difference in extrapolated values (although diversity was higher for Gulf of Oman populations for the interpolated value). For algal prey items (23S marker), prey diversity was again higher in Gulf of Oman populations of *E. pulcher* and *E. ventermaculus*, while the opposite was evident for *C. anomolus*. Overall, Gulf of Oman populations of *E. ventermaculus* ingested the highest autotroph prey diversity, followed by Arabian Gulf populations of *C. anomolus*.

We further examined the potential organismal and ecosystem-wide energetic consequences of thermal regimes and resource availability between the two locations by first assessing length-weight relationships of three co-occurring species, and then by modeling individual-based growth and mortality to estimate community-wide biomass cycling. We employed Bayesian linear models to test the effects of total length (*TL*) and *Location* on *Weight*, which showed clear effects

of *Location* across all species, with Gulf of Oman populations consistently having higher weights for a given body length (*E. ventermaculus*: *Gulf of Oman*: $\beta = 0.16$ [0.13, 0.19], *C. anomolus*: *Gulf of Oman*: $\beta = 0.15$ [0.09, 0.21], and *E. pulcher*: *Gulf of Oman*: $\beta = 0.19$ [0.14, 0.25]) (Fig. 5). Notably, empirical values for the largest individuals of *C. anomolus* from the Arabian Gulf were consistently below the model fit, suggesting worse body conditions than predicted by the model and substantially worse body conditions than Gulf of Oman individuals of comparable size (Fig 5b). In contrast, no clear differences emerged between the abundances of the three species' populations across locations (effect size uncertainties intersected zero), although *E. ventermaculus* (*Gulf of Oman*: $\beta = 0.89$ [-1.08, 2.86] and *E. pulcher* (*Gulf of Oman*: $\beta = 3.46$ [-0.42, 9.93]) showed a trend toward lower abundances in the Arabian Gulf, while *C. anomolus* exhibited the opposite trend (*Gulf of Oman*: $\beta = -0.94$ [-3.82, 1.69]).

Finally, modeling individual-based growth and mortality for cryptobenthic fish communities at each site revealed strong differences in the ecological dynamics that underpin ecosystem functioning between the Arabian Gulf and Gulf of Oman (Fig. 6). Biomass production was almost one order of magnitude higher on reefs in the Gulf of Oman (0.231 ± 0.025 [mean \pm SE] g d⁻¹ m⁻²) compared to the Arabian Gulf (0.038 ± 0.014 g d⁻¹ m⁻²), while consumed biomass was more than five times higher (0.039 ± 0.015 vs. 0.007 ± 0.001 g d⁻¹ m⁻²). Turnover was also higher in the Gulf of Oman (0.017 ± 0.005 % d⁻¹) compared to the Arabian Gulf (0.006 ± 0.005 % d⁻¹). Therefore, reefs in the two locations exhibit contrasting productivity dynamics at various levels of organization. In the Arabian Gulf, individual fishes accumulate less body mass per millimeter of body length and collectively, cryptobenthic communities produce, provide, and replenish consumer biomass at much lower rates than Gulf of Oman communities.

Discussion

As rapid environmental change sweeps across the Earth's ecosystems, garnering an understanding of the processes that underpin local community structure and ecosystem functioning is urgent. Here, we show that cryptobenthic fishes on reefs exposed to the world's most extreme temperature regime in the southeastern Arabian Gulf have reduced diversity, abundance, and body condition compared to reefs with more moderate temperatures in the nearby Gulf of Oman, despite similarities in live coral cover and benthic community structure. While species with populations in both locations exhibit thermal plasticities that enable survival in Arabian Gulf conditions, species-specific temperature tolerances are not the main driver of species presence/absence in the Arabian Gulf. Rather, poor body condition in Arabian Gulf populations suggest that physiological responses to the Arabian Gulf conditions might invoke energetic costs that can only be borne by species with low metabolic demands. Furthermore, intraspecific dietary differences indicate that cryptobenthic fishes in the Arabian Gulf need to meet these increased costs with a distinct and restricted suite of prey items. These individual energetic challenges have far reaching consequences for ecosystem-scale energy and nutrient fluxes; even conservative estimates of cryptobenthic reef fish productivity in the Arabian Gulf are an order of magnitude lower than the Gulf of Oman. Our results indicate that cryptobenthic reef fish assemblages on future coral reefs may be shaped by species-specific individual energy deficits that decrease the rate of biomass production, transfer, and renewal through small vertebrate consumers, thereby eroding a cardinal component of heterotrophic coral reef productivity (54).

Organismal responses

As the smallest and shortest-lived marine vertebrates, responses of cryptobenthic fishes to extreme temperatures should be easy to trace(50). Yet, critical thermal tolerances of all tested

species from both locations were equal to or greater than the extreme maximum summer temperatures of the southeastern Arabian Gulf (43, 45, 65). The high intrinsic tolerance of species from the relatively cool Gulf of Oman aligns with previous results of high, short-term critical thermal tolerances in cryptobenthics (43). Furthermore, swift generational turnover in cryptobenthic fishes could facilitate transgenerational thermal plasticity and increased thermal tolerance (54, 58). Collectively, this should have permitted their colonization and persistence in the geologically young southeastern Arabian Gulf (66), since no hard biogeographic boundary exists between the Gulf of Oman in the Arabian Gulf (60). Indeed, 26 out of 29 (89.7%) cryptobenthic fish species from the Gulf of Oman that were absent from the southeastern Arabian Gulf have been recorded in the cooler Arabian Gulf regions of Saudi Arabia and Kuwait (Table S1) (62, 67, 68). Thus, neither thermal tolerances to short-term temperature extremes nor biogeographic history are likely to drive the observed depauperate cryptobenthic communities on Earth's hottest coral reefs.

Instead, temperature-driven demands on an individual's energetic budget and the inability of small-bodied fishes to meet these demands appear to mediate existence on these extreme reefs. Transgenerational acclimation or adaptation of fishes to increasing temperatures can come with substantial energetic costs (39, 47, 69) that are reflected in reduced body condition (22, 70, 71). These costs are evident in the lower mass per unit body length of Arabian Gulf populations in the three examined species. Although shifts in transgenerational temperature tolerance may permit survival and adequate performance in controlled laboratory conditions (39, 47), our results show that acclimation to warmer water and its associated energetic costs may not be viable for most cryptobenthics in natural environments where they continuously engage in costly activities such as foraging and escaping predators (70).

In the southeastern Arabian Gulf, this energetic dilemma may be further exacerbated by fundamentally different dietary resources and reduced prey diversity; indeed, gut content metabarcoding revealed a different and narrower range of both primary and secondary prey resources ingested by individuals from the Arabian Gulf. Shifts in dietary composition can require changes in digestive morphology and processes that further alter species' energy budgets (72, 73), while a lower diversity of prey items can reduce individual and population persistence (74, 75). Naturally, energetic challenges would be even greater if prey in the Arabian Gulf has less favorable nutritional profiles or energy densities (76). While we did not investigate differences in diet quality (i.e., nutrient content) across locations, large reef fish species in the Arabian Gulf have been shown to ingest unusual diets dominated by nutritiously poor benthic invertebrates (77).

Moreover, the goby *Coryogalops anomolus* was the only cryptobenthic species to show weakly distinct prey composition between locations and higher autotroph prey richness in the Arabian Gulf, and it was also the only species with a higher abundance and larger body size in the Arabian Gulf as compared to the Gulf of Oman. This species also had a less pronounced reduction in body condition from the Gulf of Oman to the Arabian Gulf compared to *E. pulcher* and *E. ventermaculus*. As opposed to most dominant cryptobenthic genera in the Arabian Gulf and Gulf of Oman (e.g. *Ecsenius*, *Eviota*, *Enneapterygius*, etc.), the goby genus *Coryogalops* belongs to a clade that contains many non-reef associated species from comparatively extreme habitats (78, 79) For example, *Coryogalops* often inhabit tidepools and other shallow environments exposed to fluctuating temperatures and salinity where they rely on a sedentary lifestyle with low energetic costs (80, 81). Thus, the persistence of *C. anomolus* in the southeastern Arabian Gulf may reflect an adaptation to extreme environments afforded by its evolutionary history of belonging to a lineage of non-reef, extreme habitat specialists.

Our results indicate that species-specific capacities to cope with the energetic costs of inhabiting extreme environments, rather than the direct effects of temperature *per se* or its effect on benthic

Our results showcase an imminent threat to cryptobenthic reef fishes and their critical role for coral reef functioning: similar to corals, which are highly susceptible to extreme temperatures (27), many of the world's smallest marine ectotherms may struggle to compensate for increasing growth costs as they adapt to warming temperatures. As a consequence, small consumer productivity, energy transfer, and replenishment of biomass at the bottom of the fish food chain may severely decrease under climate change (18). Analogous to cryptobenthics, the Arabian Gulf harbors less diverse and abundant communities of large reef fishes compared to nearby locations with more moderate temperatures (102, 103). It remains unresolved whether these patterns are driven by similar mechanisms as proposed herein (e.g., the energetic filtering effect on large fish species) or relate to decreased productivity at lower trophic levels. Yet, in light of the hypothesized importance of small vertebrate consumers in global food webs (104) and the unique ecological role of cryptobenthics in coral reef trophic dynamics (54), the effects of elevated temperature on cryptobenthic fish assemblages may considerably reduce ecosystem functioning on future coral reefs.

Materials and Methods

Experimental design

We studied cryptobenthic fish communities across six distinct coral reefs in two distinct locations that dramatically differ in yearly temperature fluctuations. Sampled reefs in the Arabian Gulf (Dhabiya: 24.36383°, 54.10121°; Ras Ghanada: 24.84743°, 54.69235°; Saadiyat: 24.65771°, 54.48691°) are some of the most extreme reefs in the world in terms of the annual temperature gradient, with summer maximum temperatures reaching up to or above 36 °C, while winter minimum temperatures fall to 16 °C. In contrast, sampled reefs in the Gulf of Oman (Dibba Rock: 25.55378°, 56.35694°; Sharm Rock: 25.48229°, 56.36695°; Snoopy Rock: 25.49210°, 56.36401°) lie within more typical coral reef temperature profiles throughout the year, ranging from 32 °C to 22 °C. All fieldwork was performed in April and May of 2018.

Field sampling

We sampled six distinct reefs (hereafter *site*) in the southeastern Arabian Gulf and northwestern Gulf of Oman (three sites per location). At each site, we sampled three distinct reef outcrops for cryptobenthic reef fishes using enclosed clove oil stations (51, 105), covering an average of 4.63 ± 0.38 and 4.73 ± 0.16 m² in the Arabian Gulf and Gulf of Oman, respectively, for a total of 18 community samples. For each station, we covered a reef outcrop with a fine-mesh, bell-shaped net (2.74 m in diameter), weighted by a chain on the bottom. We then covered the same area with an impermeable bell-shaped tarpaulin, also weighted by a chain on the bottom. Then, three to four divers inoculated the area under the net with two liters of clove-oil:ethanol solution (1:5) using collapsible spray bottles (clove bud oil: Jedwards International, Inc., Braintree, MA, USA). Upon emptying the entire solution and a short wait period to allow the clove oil to disperse and take effect (approximately 2-3 mins), we removed the tarpaulin and gently peeled back the net while collecting all fishes found within the inoculated area with tweezers. We searched the entire area, including inside caves and crevices until five minutes passed without a single diver collecting any additional fishes. We placed all fishes into Ziplock bags, brought them to the surface, euthanized them with a clove-oil overdose, and immediately placed them into an ice-water slurry until processing and preservation. At the end of each day, all specimens were brought to the laboratory at NYUAD or to room #211 at the Radisson Blu hotel in Fujairah. To quantify benthic community structure, we used a haphazardly placed 20×20cm PVC-quadrat to frame and take five photographs of the benthos at each sampled outcrop.

In addition to the quantitative samples obtained from the clove-oil stations, we collected cryptobenthic fish individuals for thermal tolerance trials using roving diver collections. Specifically, two divers, each equipped with spray bottles of clove-oil:ethanol solution, a dipnet, and Ziplock bags, searched the reef for cryptobenthic fishes across three species in the Arabian Gulf (*Coryogalops anomolus*, *Ecsenius pulcher*, and *Enneapterygius ventermaculus*) and six species in the Gulf of Oman (*C. anomolus*, *E. pulcher*, and *E. ventermaculus* plus *Eviota guttata*, *Helcogramma fuscipinna*, and *Heteroleotris vulgaris*). Upon locating an individual or identifying a suitable microhabitat in which a fish was suspected, the diver applied the clove-oil solution until the fish showed signs of anesthesia. At the earliest opportunity, we caught the fish with a dipnet and placed it into a ziplock bag. Upon completion of the dive, all fishes were placed in small holding tanks equipped with air stones and periodically replenished with fresh seawater. Upon completion of all collections, fishes were brought to the seawater laboratory facilities at NYUAD. All roving diver collections were performed at Dhabiya Reef (Arabian Gulf) and Snoopy Rock (Gulf of Oman).

Laboratory processing

For samples obtained from the enclosed clove-oil stations, we followed an established protocol that involved photographing, identifying, recording, measuring, weighing and preserving each specimen (51). To photograph the fishes, we placed each individual in a small photo tank and used a Nikon D300 DSLR camera with an AF-S Micro Nikkor 60mm macro lens (f/2.8G ED; Nikon Inc., Melville, NY, USA) against a black or white background. We measured each individual to the nearest 0.1mm using digital calipers and weighed the individual (wet weight) to the nearest 0.001 grams on a precision jewelry scale. We preserved all individuals in 95% ethanol, either separately or in lots with conspecifics. A subset of the samples was shipped to the University of Washington Fish Collection, where they were cataloged, while the rest were retained and archived at NYUAD.

Benthic photo analysis

For the benthic photographs, we created a grid with 16 equally spaced points which we superimposed on every photograph. We then categorized the benthos at each of the points into functional groups, including barnacles, bleached corals, crustose coralline algae, dead coral, hydroids, branching, encrusting, foliose, and massive live coral, mollusks, bare rock, soft sediment, sponges, algal turf, and sea urchins. Whenever visual identification was not possible (due to obstruction, shading, or blurriness), we categorized the point as “unidentifiable” (n = 69 out of 1,440). All photographs with the grid superimposed will be made accessible with the raw data of the paper.

Critical thermal maximum and minimum trials

We examined individual temperature tolerances by using critical thermal maximum (CT_{max}) and minimum (CT_{min}) trials (106). We transported all fishes caught during roving diver collections to the wet laboratory facilities at NYUAD and housed them for at least 48 hours in large holding tanks. Trials took place from the 9th to 13th of May of 2018. For the trials, a haphazardly selected subset of individuals was moved from the holding tanks into separate chambers filled with seawater at ambient temperature and salinity. Then, after providing individuals with a 15-minute settlement period, we incrementally decreased (CT_{min}) or increased (CT_{max}) the water temperature within the chambers while keeping all other parameters constant. Specifically, we lowered or

Genohub service provider (Austin, Texas, USA). Prior to sequencing, quality control measures were performed, including bead cleaning with Agencourt AMPure XP beads (Beckman Coulter, Brea, California, USA) to remove <200 bp amplicons, sample quantification with a Qubit Fluorometer (Invitrogen, Carlsbad, California, USA), and amplicon average size analysis with an Agilent TapeStation 4200 (Agilent, Santa Clara, California, USA). Finally, sequencing was performed on an Illumina HiSeq using the HiSeq Rapid SBS Kit v2, 500-cycles (Illumina, San Diego, California, USA).

511

512 *Sequence bioinformatics*

513 For the COI sequences, a joint QIIME (112) and UPARSE (113) pipeline was employed for
514 bioinformatic processing. Sequences were demultiplexed and initial quality filtering was
515 performed with QIIME v1.9.1. Primer sequences were trimmed with Cutadapt v1.18 (114), then
516 forward and reverse reads were pair-end merged with USEARCH v11.0.667 (115). Quality
517 filtering was then performed in accordance with the UPARSE pipeline. Sequences were clustered
518 into operational taxonomic units (OTUs) at 99% similarity, and the OTU table was generated by
519 mapping quality-filtered reads back to the OTU seeds. Taxonomy was assigned to OTUs by
520 recording the top basic local alignment search tool (BLASTn (116)) hit when query coverage and
521 percent identity exceeded 95% and 80%, respectively. GenBank was used as the reference
522 database. When OTU taxonomic assignments did not meet these criteria, taxonomy was removed
523 and recorded as “NA.” Finally, we removed all self-hits from the OTU-dataset, which we
524 identified by matching the highest sequence reads of each species to its individuals, as well as
525 unambiguous (>97% identity match) assignments to species not found in the geographic region
526 (specifically *Oncorhynchus nerka*).

527 For the 23S sequences, raw sequences were processed with the JAMP pipeline
528 (<https://github.com/VascoElbrecht/JAMP>). After demultiplexing, forward and reverse reads were
529 pair-end merged with USEARCH v11.0.667 (115). Primers were trimmed from both ends using
530 Cutadapt v1.18 (114), and quality filtering was conducted with expected error filtering, as
531 implemented through USEARCH (117). Reads affected by sequencing and PCR error were
532 removed using the UNOISE algorithm (118). Exact sequence variants (ESVs) were then compiled
533 into an ESV table, which included read counts for each sample. Taxonomy was assigned to each
534 ESV by mapping them against a 23S database from Silva (119), specifying zero deviations to
535 ensure mapping accuracy. Consensus taxonomy was generated from the hit tables, first
536 considering 100% matches, then decreasing by 1% until hits were available for each ESV.
537 Taxonomy that was present in at least 90% of the hits was reported; otherwise, an “NA” was
538 assigned when several different taxa matched the ESV. For error reduction due to misidentified
539 taxa, the bracket was increased to 2% when matches of 97% and higher were present, but no
540 family-level or lower taxonomy was assigned.

541

542 *Statistical analysis and modeling*

543 To analyze the community variables, we first calculated the surface area (SA) for each sampled
544 outcrop from the curved surface length (CSL) by deriving the sampled outcrop’s radius r ($r =$
545 $2 \cdot \text{CSL} / 2\pi$), then computing available surface area under the assumption that outcrops are
546 hemispherical constructs ($SA = 4\pi r^2 / 2$). We calculated the sum of individuals, species, and their
547 respective body weight for each station to obtain abundance, diversity, and biomass estimates,
548 which we converted to density estimates by dividing them by the sampled surface area. Using
549 these estimates, we performed three Bayesian hierarchical models, each on the natural logarithm
550 of the response variables (species density, individual density, and biomass per m²). Models were

We examined prey item ingestion of the examined fishes using a network theory approach for both the COI and 23S markers (121). We first created a presence-absence matrix of OTUs/ESVs across fish individuals in all species and their populations, creating a bipartite dietary network based on prey presence or absence. To examine the community structure within the network, we omitted all prey items with only a single occurrence across the dataset since the full dataset identified the majority of individuals as unique modules. This step reduced the COI dataset from 1,357 to 1,046 unique predator-prey interactions and the 23S dataset from 7,872 to 5,698 predator-prey interactions. We then sought to identify modules within the network using Newman's modularity measure (122). We used Beckett's community detection algorithm (123), which we re-iterated 20 times for each dataset. We then used the convergent output from the 20 iterations to determine the module membership of each individual in our network. We then created a data frame from the original presence-absence matrix that contained each OTU/ESV and its linkage to the fish individual in two columns, which we then summarized by the respective modules. This created a list of symbolic edges in the network across the two columns, linking each prey item to a module, which we plotted as a bipartite dietary network tree using the Fruchterman-Reingold algorithm. We also plotted module membership in a mosaic plot.

Furthermore, for the COI and 23S markers, we investigated prey item diversity ingested by each species' population by producing interpolated and extrapolated rarefaction curves, which showcase sequencing depth by plotting prey item species richness by the total number of sequences detected for each species. We ran rarefaction analyses by rarefying species richness estimates for each species or population to an endpoint defined by the maximum sequences in any population using 100 bootstraps and 50 knots along the x-axis (124).

Finally, we modelled growth and mortality dynamics in cryptobenthic fish assemblages from the two locations, ultimately yielding a standing biomass estimate and three rate-based metrics that serve as indicators of energy and nutrient fluxes, thus indicating ecosystem functioning(25): produced biomass (in g d⁻¹m⁻²), consumed biomass (in g d⁻¹m⁻²), and total turnover (percent d⁻¹) (94, 125, 126). Produced biomass represents the amount of fish tissue accumulated by an assemblage (in this case, a cryptobenthic fish assemblage collected in a given sample), thus considering only the growth that will occur on any given day (based on yearly averages in this case). Consumed biomass represents the amount of fish tissue that perished based on our estimates of fish mortality. In this pathway, the energy and nutrients produced by fishes are provided to other consumers or decomposers via predation or detritivory. Finally, total turnover expands on the classic estimate of turnover (the production/standing biomass [P/B] ratio (127)) by also including consumed biomass (consumed biomass/standing biomass) (125). As such, the turnover metric approximates the rate at which particles flow through the system, either via incorporation into fish biomass or release to other consumers through mortality.

For the modeling, we first accrued species-specific information on maximum lengths and a range of coarse ecological traits (pertaining to diet, sociality, habitat association, and prevailing mean sea surface temperatures [SST]) from the literature for each species in our samples. We also extracted length-weight relationships at the family-level, since not all species in our samples were common enough to construct robust length-weight relationships. We then used these data to calculate species-specific growth coefficients (K_{max}) to the specified maximum size and modeled individual weight gain based on changes in fish size per day under a Von Bertalanffy Growth Model (VBGM) (126). By subtracting the observed fish size (as obtained from our samples) from the weight obtained by the same fish after one day (from the model), we calculated the expected biomass production by that individual. We estimated daily mortality rates by calculating species-level mortality risk coefficients via VBGM parameters and SST (125, 128), and then we adjusted the risk based on relationships between mortality and body size (129). Using these coefficients, we obtained a daily survival probability for a given individual in the dataset. By combining this

probability with biomass production as obtained from the previous step, we were able to generate the expected loss of biomass due to natural mortality at the individual level. Finally, we summed the individual-level estimates of weight, growth, and mortality for each sample to obtain community-level values of standing biomass, produced biomass, and consumed biomass, which we used to calculate total turnover as the combined quotients of produced and consumed biomass and standing biomass.

All data preparation, analyses, and visualizations were performed in *R* (130) (version 3.6.1) using the *tidyverse* (131), *vegan* (132), *brms* (120), *iNEXT* (124), *igraph* (133), *bipartite* (134), *tidybayes* (135), *xgboost* (136), *emmeans* (137), *oceanmap* (138), *ncdf4* (139) and *raster* (140) packages. All graphs were made using the *Trimma lantana* and *Coryphaena hippurus* color palettes in the package *fishualize* (141). Growth modeling was performed using a beta version of the package *rfishprod*.

H2: Supplementary Materials

- Fig. S1. Rarefaction curves of OTU and ESV richness
- Table S1. Presence, abundance, and previous records of species
- Table S2. Contrasts between levels of the explanatory variable for the model testing CT_{max} differences in cryptobenthic reef fishes.
- Table S3. Contrasts between levels of the explanatory variable for the model testing CT_{min} differences in cryptobenthic reef fishes.
- Material S1: Raw data and code

References and Notes

1. M. Dornelas, N. J. Gotelli, B. McGill, H. Shimadzu, F. Moyes, C. Sievers, A. E. Magurran, Assemblage time series reveal biodiversity change but not systematic loss. *Science*. **344**, 296–299 (2014).
2. S. A. Blowes, S. R. Supp, L. H. Antão, A. Bates, H. Bruelheide, J. M. Chase, F. Moyes, A. Magurran, B. McGill, I. H. Myers-Smith, The geography of biodiversity change in marine and terrestrial assemblages. *Science*. **366**, 339–345 (2019).
3. C. N. Johnson, A. Balmford, B. W. Brook, J. C. Buettel, M. Galetti, L. Guangchun, J. M. Wilmschurst, Biodiversity losses and conservation responses in the Anthropocene. *Science*. **356**, 270–275 (2017).
4. G. M. Mace, K. Norris, A. H. Fitter, Biodiversity and ecosystem services: a multilayered relationship. *Trends in ecology & evolution*. **27**, 19–26 (2012).
5. M. Vellend, *The theory of ecological communities (MPB-57)* (Princeton University Press, 2016), vol. 75.
6. N. J. Kraft, P. B. Adler, O. Godoy, E. C. James, S. Fuller, J. M. Levine, Community assembly, coexistence and the environmental filtering metaphor. *Functional Ecology*. **29**, 592–599 (2015).
7. N. J. Kraft, R. Valencia, D. D. Ackerly, Functional traits and niche-based tree community assembly in an Amazonian forest. *Science*. **322**, 580–582 (2008).

- 694 8. M. A. Leibold, M. Holyoak, N. Mouquet, P. Amarasekare, J. M. Chase, M. F. Hoopes, R.
695 D. Holt, J. B. Shurin, R. Law, D. Tilman, The metacommunity concept: a framework for
696 multi-scale community ecology. *Ecology letters*. **7**, 601–613 (2004).
- 697 9. B. J. Cardinale, J. E. Duffy, A. Gonzalez, D. U. Hooper, C. Perrings, P. Venail, A.
698 Narwani, G. M. Mace, D. Tilman, D. A. Wardle, Biodiversity loss and its impact on
699 humanity. *Nature*. **486**, 59–67 (2012).
- 700 10. J. E. Duffy, C. M. Godwin, B. J. Cardinale, Biodiversity effects in the wild are common
701 and as strong as key drivers of productivity. *Nature*. **549**, 261 (2017).
- 702 11. A. K. Schweiger, J. Cavender-Bares, P. A. Townsend, S. E. Hobbie, M. D. Madritch, R.
703 Wang, D. Tilman, J. A. Gamon, Plant spectral diversity integrates functional and
704 phylogenetic components of biodiversity and predicts ecosystem function. *Nature ecology
705 & evolution*. **2**, 976 (2018).
- 706 12. G. T. Pecl, M. B. Araújo, J. D. Bell, J. Blanchard, T. C. Bonebrake, I.-C. Chen, T. D. Clark,
707 R. K. Colwell, F. Danielsen, B. Evengård, Biodiversity redistribution under climate
708 change: Impacts on ecosystems and human well-being. *Science*. **355**, eaai9214 (2017).
- 709 13. B. R. Scheffers, L. De Meester, T. C. Bridge, A. A. Hoffmann, J. M. Pandolfi, R. T.
710 Corlett, S. H. Butchart, P. Pearce-Kelly, K. M. Kovacs, D. Dudgeon, The broad footprint of
711 climate change from genes to biomes to people. *Science*. **354**, aaf7671 (2016).
- 712 14. F. C. García, E. Bestion, R. Warfield, G. Yvon-Durocher, Changes in temperature alter the
713 relationship between biodiversity and ecosystem functioning. *Proceedings of the National
714 Academy of Sciences*. **115**, 10989–10994 (2018).
- 715 15. H. O. Pörtner, A. P. Farrell, Physiology and climate change. *Science*. **322**, 690–692 (2008).
- 716 16. C. Deutsch, A. Ferrel, B. Seibel, H.-O. Pörtner, R. B. Huey, Climate change tightens a
717 metabolic constraint on marine habitats. *Science*. **348**, 1132–1135 (2015).
- 718 17. F. Bozinovic, H. Pörtner, Physiological ecology meets climate change. *Ecology and
719 evolution*. **5**, 1025–1030 (2015).
- 720 18. D. R. Barneche, M. Jahn, F. Seebacher, Warming increases the cost of growth in a model
721 vertebrate. *Functional Ecology*.
- 722 19. J. H. Brown, C. A. Hall, R. M. Sibly, Equal fitness paradigm explained by a trade-off
723 between generation time and energy production rate. *Nature ecology & evolution*. **2**, 262
724 (2018).
- 725 20. A. Toseland, S. J. Daines, J. R. Clark, A. Kirkham, J. Strauss, C. Uhlig, T. M. Lenton, K.
726 Valentin, G. A. Pearson, V. Moulton, The impact of temperature on marine phytoplankton
727 resource allocation and metabolism. *Nature Climate Change*. **3**, 979 (2013).
- 728 21. D. R. Barneche, A. P. Allen, The energetics of fish growth and how it constrains food-web
729 trophic structure. *Ecology letters*. **21**, 836–844 (2018).
- 730 22. J. L. Gardner, A. Peters, M. R. Kearney, L. Joseph, R. Heinsohn, Declining body size: a
731 third universal response to warming? *Trends in ecology & evolution*. **26**, 285–291 (2011).

23. P. Chesson, Mechanisms of maintenance of species diversity. *Annual review of Ecology and Systematics*. **31**, 343–366 (2000).
24. A. D. Barnes, M. Jochum, J. S. Lefcheck, N. Eisenhauer, C. Scherber, M. I. O'Connor, P. de Ruiter, U. Brose, Energy flux: the link between multitrophic biodiversity and ecosystem functioning. *Trends in ecology & evolution*. **33**, 186–197 (2018).
25. S. J. Brandl, D. B. Rasher, I. M. Côté, J. M. Casey, E. S. Darling, J. S. Lefcheck, J. E. Duffy, Coral reef ecosystem functioning: eight core processes and the role of biodiversity. *Frontiers in Ecology and the Environment* (2019).
26. M. Spalding, L. Burke, S. A. Wood, J. Ashpole, J. Hutchison, P. zu Ermgassen, Mapping the global value and distribution of coral reef tourism. *Marine Policy*. **82**, 104–113 (2017).
27. T. P. Hughes, K. D. Anderson, S. R. Connolly, S. F. Heron, J. T. Kerry, J. M. Lough, A. H. Baird, J. K. Baum, M. L. Berumen, T. C. Bridge, Spatial and temporal patterns of mass bleaching of corals in the Anthropocene. *Science*. **359**, 80–83 (2018).
28. M. S. Pratchett, A. S. Hoey, S. K. Wilson, V. Messmer, N. A. Graham, Changes in biodiversity and functioning of reef fish assemblages following coral bleaching and coral loss. *Diversity*. **3**, 424–452 (2011).
29. S. J. Brandl, M. J. Emslie, D. M. Ceccarelli, Habitat degradation increases functional originality in highly diverse coral reef fish assemblages. *Ecosphere*. **7** (2016).
30. L. Fontoura, K. J. Zawada, S. D'agata, A. H. Baird, M. Álvarez-Noriega, R. M. Woods, O. J. Luiz, M. Dornelas, J. S. Madin, J. M. Maina, Climate-driven shift in coral morphological structure predicts decline of juvenile reef fishes. *Global change biology* (2019).
31. D. R. Bellwood, A. S. Hoey, J. L. Ackerman, M. Depczynski, Coral bleaching, reef fish community phase shifts and the resilience of coral reefs. *Global Change Biology*. **12**, 1587–1594 (2006).
32. J. P. Robinson, S. K. Wilson, J. Robinson, C. Gerry, J. Lucas, C. Assan, R. Govinden, S. Jennings, N. A. Graham, Productive instability of coral reef fisheries after climate-driven regime shifts. *Nature ecology & evolution*. **3**, 183 (2019).
33. S. Wismer, S. B. Tebbett, R. P. Streit, D. R. Bellwood, Young fishes persist despite coral loss on the Great Barrier Reef. *Communications Biology*. **2**, 456 (2019).
34. B. M. Taylor, C. E. Benkwitt, H. Choat, K. D. Clements, N. A. Graham, M. G. Meekan, Synchronous biological feedbacks in parrotfishes associated with pantropical coral bleaching. *Global Change Biology* (2019).
35. H. O. Pörtner, R. Knust, Climate change affects marine fishes through the oxygen limitation of thermal tolerance. *science*. **315**, 95–97 (2007).
36. L. Comte, J. D. Olden, Climatic vulnerability of the world's freshwater and marine fishes. *Nature Climate Change*. **7**, 718 (2017).

37. P. L. Munday, M. I. McCormick, G. E. Nilsson, Impact of global warming and rising CO₂ levels on coral reef fishes: what hope for the future? *Journal of Experimental Biology*. **215**, 3865–3873 (2012).
38. P. L. Munday, G. P. Jones, M. S. Pratchett, A. J. Williams, Climate change and the future for coral reef fishes. *Fish and Fisheries*. **9**, 261–285 (2008).
39. J. Donelson, P. Munday, M. McCormick, C. Pitcher, Rapid transgenerational acclimation of a tropical reef fish to climate change. *Nature Climate Change*. **2**, 30 (2012).
40. J. Johansen, G. Jones, Increasing ocean temperature reduces the metabolic performance and swimming ability of coral reef damselfishes. *Global Change Biology*. **17**, 2971–2979 (2011).
41. J. L. Rummer, C. S. Couturier, J. A. Stecyk, N. M. Gardiner, J. P. Kinch, G. E. Nilsson, P. L. Munday, Life on the edge: thermal optima for aerobic scope of equatorial reef fishes are close to current day temperatures. *Global change biology*. **20**, 1055–1066 (2014).
42. G. E. Nilsson, N. Crawley, I. G. Lunde, P. L. Munday, Elevated temperature reduces the respiratory scope of coral reef fishes. *Global Change Biology*. **15**, 1405–1412 (2009).
43. J. Eme, W. A. Bennett, Critical thermal tolerance polygons of tropical marine fishes from Sulawesi, Indonesia. *Journal of Thermal Biology*. **34**, 220–225 (2009).
44. N. M. Gardiner, P. L. Munday, G. E. Nilsson, Counter-gradient variation in respiratory performance of coral reef fishes at elevated temperatures. *PLoS One*. **5**, e13299 (2010).
45. C. Mora, A. Ospina, Tolerance to high temperatures and potential impact of sea warming on reef fishes of Gorgona Island (tropical eastern Pacific). *Marine Biology*. **139**, 765–769 (2001).
46. D. A. Feary, M. S. Pratchett, M. J. Emslie, A. M. Fowler, W. F. Figueira, O. J. Luiz, Y. Nakamura, D. J. Booth, Latitudinal shifts in coral reef fishes: why some species do and others do not shift. *Fish and Fisheries*. **15**, 593–615 (2014).
47. M. A. Bernal, J. M. Donelson, H. D. Veilleux, T. Ryu, P. L. Munday, T. Ravasi, Phenotypic and molecular consequences of stepwise temperature increase across generations in a coral reef fish. *Molecular Ecology*. **27**, 4516–4528 (2018).
48. M. Grenchik, J. Donelson, P. Munday, Evidence for developmental thermal acclimation in the damselfish, *Pomacentrus moluccensis*. *Coral Reefs*. **32**, 85–90 (2013).
49. D. D. Miller, Y. Ota, U. R. Sumaila, A. M. Cisneros-Montemayor, W. W. Cheung, Adaptation strategies to climate change in marine systems. *Global change biology*. **24**, e1–e14 (2018).
50. S. J. Brandl, C. H. Goatley, D. R. Bellwood, L. Tornabene, The hidden half: ecology and evolution of cryptobenthic fishes on coral reefs. *Biological Reviews*. **93**, 1846–1873 (2018).
51. S. J. Brandl, J. M. Casey, N. Knowlton, J. E. Duffy, Marine dock pilings foster diverse, native cryptobenthic fish assemblages across bioregions. *Ecology and evolution*. **7**, 7069–7079 (2017).

- 806 52. G. N. Ahmadi, L. Tornabene, D. J. Smith, F. L. Pezold, The relative importance of
807 regional, local, and evolutionary factors structuring cryptobenthic coral-reef assemblages.
808 *Coral Reefs*. **37**, 279–293 (2018).
- 809 53. D. J. Coker, J. D. DiBattista, T. H. Sinclair-Taylor, M. L. Berumen, Spatial patterns of
810 cryptobenthic coral-reef fishes in the Red Sea. *Coral Reefs*, 1–7 (2017).
- 811 54. S. J. Brandl, L. Tornabene, C. H. Goatley, J. M. Casey, R. A. Morais, I. M. Côté, C. C.
812 Baldwin, V. Parravicini, N. M. Schiettekatte, D. R. Bellwood, Demographic dynamics of
813 the smallest marine vertebrates fuel coral reef ecosystem functioning. *Science*. **364**, 1189–
814 1192 (2019).
- 815 55. P. J. Miller, (Oxford University Press, 1996), vol. 69.
- 816 56. M. Depczynski, D. Bellwood, Microhabitat utilisation patterns in cryptobenthic coral reef
817 fish communities. *Marine Biology*. **145**, 455–463 (2004).
- 818 57. D. R. Bellwood, A. H. Baird, M. Depczynski, A. González-Cabello, A. S. Hoey, C. D.
819 Lefèvre, J. K. Tanner, Coral recovery may not herald the return of fishes on damaged coral
820 reefs. *Oecologia*. **170**, 567–573 (2012).
- 821 58. M. Depczynski, D. R. Bellwood, Shortest recorded vertebrate lifespan found in a coral reef
822 fish. *Current Biology*. **15**, R288–R289.
- 823 59. L. Tornabene, S. Valdez, M. Erdmann, F. Pezold, Support for a ‘Center of Origin’ in the
824 Coral Triangle: Cryptic diversity, recent speciation, and local endemism in a diverse
825 lineage of reef fishes (Gobiidae: Eviota). *Molecular phylogenetics and evolution*. **82**, 200–
826 210 (2015).
- 827 60. A. Price, C. Sheppard, C. Roberts, The Gulf: its biological setting. *Marine Pollution*
828 *Bulletin*. **27**, 9–15 (1993).
- 829 61. B. M. Riegl, S. J. Purkis, in *Coral reefs of the Gulf* (Springer, 2012), pp. 1–4.
- 830 62. S. Eagderi, R. Fricke, H. Esmaeili, P. Jalili, Annotated checklist of the fishes of the Persian
831 Gulf: Diversity and conservation status. *Iranian Journal of Ichthyology*. **6**, 1–171 (2019).
- 832 63. J. M. Casey, C. P. Meyer, F. Morat, S. J. Brandl, S. Planes, V. Parravicini, Reconstructing
833 hyperdiverse food webs: Gut content metabarcoding as a tool to disentangle trophic
834 interactions on coral reefs. *Methods in Ecology and Evolution*. **10**, 1157–1170 (2019).
- 835 64. M. Depczynski, D. R. Bellwood, The role of cryptobenthic reef fishes in coral reef
836 trophodynamics. *Marine Ecology Progress Series*. **256**, 183–191 (2003).
- 837 65. M. S. Pratchett, S. K. Wilson, P. L. Munday, 13 Effects of climate change on coral reef
838 fishes. *Ecology of fishes on coral reefs*, 127 (2015).
- 839 66. S. J. Purkis, B. M. Riegl, in *Coral Reefs of the Gulf: Adaptation to Climatic Extremes*, B.
840 M. Riegl, S. J. Purkis, Eds. (Springer Netherlands, Dordrecht, 2012;
841 https://doi.org/10.1007/978-94-007-3008-3_3), pp. 33–50.

- 842 67. F. Krupp, T. Müller, The status of fish populations in the northern Arabian Gulf two years
843 after the 1991 Gulf War oil spill. *Courier Forschungsinst Senckenb.* **166**, 67–75 (1994).
- 844 68. J. Bishop, History and current checklist of Kuwait’s ichthyofauna. *Journal of Arid*
845 *Environments.* **54**, 237–256 (2003).
- 846 69. J. M. Donelson, P. L. Munday, M. I. McCORMICK, G. E. Nilsson, Acclimation to
847 predicted ocean warming through developmental plasticity in a tropical reef fish. *Global*
848 *Change Biology.* **17**, 1712–1719 (2011).
- 849 70. J. Ohlberger, Climate warming and ectotherm body size—from individual physiology to
850 community ecology. *Functional Ecology.* **27**, 991–1001 (2013).
- 851 71. J. Peig, A. J. Green, The paradigm of body condition: a critical reappraisal of current
852 methods based on mass and length. *Functional Ecology.* **24**, 1323–1332 (2010).
- 853 72. K. E. Sullam, C. M. Dalton, J. A. Russell, S. S. Kilham, R. El-Sabaawi, D. P. German, A.
854 S. Flecker, Changes in digestive traits and body nutritional composition accommodate a
855 trophic niche shift in Trinidadian guppies. *Oecologia.* **177**, 245–257 (2015).
- 856 73. C. J. Whelan, J. S. Brown, K. A. Schmidt, B. B. Steele, M. F. Willson, Linking consumer–
857 resource theory and digestive physiology: application to diet shifts. *Evolutionary Ecology*
858 *Research.* **2**, 911–934 (2000).
- 859 74. O. L. Petchey, Prey diversity, prey composition, and predator population dynamics in
860 experimental microcosms. *Journal of Animal Ecology.* **69**, 874–882 (2000).
- 861 75. R. L. Merrick, M. K. Chumbley, G. V. Byrd, Diet diversity of Steller sea lions (*Eumetopias*
862 *jubatus*) and their population decline in Alaska: a potential relationship. *Can. J. Fish.*
863 *Aquat. Sci.* **54**, 1342–1348 (1997).
- 864 76. D. W. Hondorp, S. A. Pothoven, S. B. Brandt, Influence of *Diporeia* density on diet
865 composition, relative abundance, and energy density of planktivorous fishes in southeast
866 Lake Michigan. *Transactions of the American fisheries Society.* **134**, 588–601 (2005).
- 867 77. R. Shraim, M. M. Dieng, M. Vinu, G. Vaughan, D. McParland, Y. Idaghdour, J. A. Burt,
868 Environmental Extremes Are Associated with Dietary Patterns in Arabian Gulf Reef
869 Fishes. *Frontiers in Marine Science.* **4**, 285 (2017).
- 870 78. A. Agorreta, D. San Mauro, U. Schliewen, J. L. Van Tassell, M. Kovačić, R. Zardoya, L.
871 Rüber, Molecular phylogenetics of Gobioidae and phylogenetic placement of European
872 gobies. *Molecular Phylogenetics and Evolution.* **69**, 619–633 (2013).
- 873 79. C. E. Thacker, D. M. Roje, Phylogeny of Gobiidae and identification of gobiid lineages.
874 *Systematics and Biodiversity.* **9**, 329–347 (2011).
- 875 80. M. Kovačić, S. V. Bogorodsky, A. O. Mal, Two new species of *Coryogalops* (Perciformes:
876 Gobiidae) from the Red Sea. *Zootaxa.* **3881**, 513–531 (2014).
- 877 81. Rishworth GM, Strydom NA, Perissinotto R, Fishes associated with living stromatolite
878 communities in peritidal pools: predators, recruits and ecological traps. *Mar Ecol Prog Ser.*
879 **580**, 153–167 (2017).

880 82. P. L. Munday, G. P. Jones, The ecological implications of small body size among coral-reef
881 fishes. *Oceanogr Mar Biol Annu Rev.* **36**, 373–411 (1998).

882 83. E. Sandblom, T. D. Clark, A. Gräns, A. Ekström, J. Brijs, L. F. Sundström, A. Odelström,
883 A. Adill, T. Aho, F. Jutfelt, Physiological constraints to climate warming in fish follow
884 principles of plastic floors and concrete ceilings. *Nature communications.* **7**, 11447 (2016).

885 84. T. Norin, N. B. Metcalfe, Ecological and evolutionary consequences of metabolic rate
886 plasticity in response to environmental change. *Philosophical Transactions of the Royal*
887 *Society B.* **374**, 20180180 (2019).

888 85. K. S. Sheldon, S. Yang, J. J. Tewksbury, Climate change and community disassembly:
889 impacts of warming on tropical and temperate montane community structure. *Ecology*
890 *Letters.* **14**, 1191–1200 (2011).

891 86. C. Crossland, B. Hatcher, S. Smith, Role of coral reefs in global ocean production. *Coral*
892 *reefs.* **10**, 55–64 (1991).

893 87. J. M. Gove, M. A. McManus, A. B. Neuheimer, J. J. Polovina, J. C. Drazen, C. R. Smith,
894 M. A. Merrifield, A. M. Friedlander, J. S. Ehses, C. W. Young, Near-island biological
895 hotspots in barren ocean basins. *Nature communications.* **7**, 10581 (2016).

896 88. J. M. De Goeij, D. Van Oevelen, M. J. Vermeij, R. Osinga, J. J. Middelburg, A. F. de
897 Goeij, W. Admiraal, Surviving in a marine desert: the sponge loop retains resources within
898 coral reefs. *Science.* **342**, 108–110 (2013).

899 89. C. Wild, M. Huettel, A. Klueter, S. G. Kremb, M. Y. Rasheed, B. B. Jørgensen, Coral
900 mucus functions as an energy carrier and particle trap in the reef ecosystem. *Nature.* **428**,
901 66–70 (2004).

902 90. W. Hamner, M. Jones, J. Carleton, I. Hauri, D. M. Williams, Zooplankton, planktivorous
903 fish, and water currents on a windward reef face: Great Barrier Reef, Australia. *Bulletin of*
904 *Marine Science.* **42**, 459–479 (1988).

905 91. B. G. Hatcher, Coral reef primary productivity: a beggar’s banquet. *Trends in Ecology &*
906 *Evolution.* **3**, 106–111 (1988).

907 92. P. Bacon, W. Gurney, W. Jones, I. McLaren, A. Youngson, Seasonal growth patterns of
908 wild juvenile fish: partitioning variation among explanatory variables, based on individual
909 growth trajectories of Atlantic salmon (*Salmo salar*) parr. *Journal of Animal Ecology.* **74**,
910 1–11 (2005).

911 93. S. L. Coles, Coral species diversity and environmental factors in the Arabian Gulf and the
912 Gulf of Oman: a comparison to the Indo-Pacific region. *Atoll Research Bulletin* (2003).

913 94. R. A. Morais, D. R. Bellwood, Pelagic Subsidies Underpin Fish Productivity on a
914 Degraded Coral Reef. *Current Biology.* **29**, 1521–1527 (2019).

915 95. B. Riegl, Effects of the 1996 and 1998 positive sea-surface temperature anomalies on
916 corals, coral diseases and fish in the Arabian Gulf (Dubai, UAE). *Marine biology.* **140**, 29–
917 40 (2002).

- 918 96. B. Riegl, S. Purkis, Coral population dynamics across consecutive mass mortality events.
919 *Global change biology*. **21**, 3995–4005 (2015).
- 920 97. J. Burt, S. Al-Harthi, A. Al-Cibahy, Long-term impacts of coral bleaching events on the
921 world's warmest reefs. *Marine environmental research*. **72**, 225–229 (2011).
- 922 98. J. A. Burt, F. Paparella, N. Al-Mansoori, A. Al-Mansoori, H. Al-Jailani, Causes and
923 consequences of the 2017 coral bleaching event in the southern Persian/Arabian Gulf.
924 *Coral Reefs*. **38**, 567–589 (2019).
- 925 99. D. J. Coker, S. K. Wilson, M. S. Pratchett, Importance of live coral habitat for reef fishes.
926 *Reviews in Fish Biology and Fisheries*. **24**, 89–126 (2014).
- 927 100. M. S. Pratchett, A. H. Baird, A. G. Bauman, J. A. Burt, Abundance and composition of
928 juvenile corals reveals divergent trajectories for coral assemblages across the United Arab
929 Emirates. *Marine Pollution Bulletin*. **114**, 1031–1035 (2017).
- 930 101. P. L. Munday, Habitat loss, resource specialization, and extinction on coral reefs. *Global*
931 *Change Biology*. **10**, 1642–1647 (2004).
- 932 102. J. A. Burt, D. A. Feary, A. G. Bauman, P. Usseglio, G. H. Cavalcante, P. F. Sale,
933 Biogeographic patterns of reef fish community structure in the northeastern Arabian
934 Peninsula. *ICES Journal of Marine Science*. **68**, 1875–1883 (2011).
- 935 103. D. A. Feary, J. A. Burt, G. H. Cavalcante, A. G. Bauman, in *Coral Reefs of the Gulf:*
936 *Adaptation to Climatic Extremes*, B. M. Riegl, S. J. Purkis, Eds. (Springer Netherlands,
937 Dordrecht, 2012; https://doi.org/10.1007/978-94-007-3008-3_9), pp. 163–170.
- 938 104. U. Brose, P. Archambault, A. D. Barnes, L.-F. Bersier, T. Boy, J. Canning-Clode, E. Conti,
939 M. Dias, C. Digel, A. Dissanayake, Predator traits determine food-web architecture across
940 ecosystems. *Nature ecology & evolution*. **3**, 919 (2019).
- 941 105. J. L. Ackerman, D. R. Bellwood, Reef fish assemblages: a re-evaluation using enclosed
942 rotenone stations. *Marine Ecology-Progress Series*. **206**, 227–237 (2000).
- 943 106. T. L. Beitingner, W. A. Bennett, R. W. McCauley, Temperature tolerances of North
944 American freshwater fishes exposed to dynamic changes in temperature. *Environmental*
945 *biology of fishes*. **58**, 237–275 (2000).
- 946 107. M. Leray, J. Y. Yang, C. P. Meyer, S. C. Mills, N. Agudelo, V. Ranwez, J. T. Boehm, R. J.
947 Machida, A new versatile primer set targeting a short fragment of the mitochondrial COI
948 region for metabarcoding metazoan diversity: application for characterizing coral reef fish
949 gut contents. *Frontiers in zoology*. **10**, 34 (2013).
- 950 108. J. Geller, C. Meyer, M. Parker, H. Hawk, Redesign of PCR primers for mitochondrial
951 cytochrome c oxidase subunit I for marine invertebrates and application in all-taxa biotic
952 surveys. *Molecular ecology resources*. **13**, 851–861 (2013).
- 953 109. A. R. Sherwood, G. G. Presting, Universal primers amplify a 23S rDNA plastid marker in
954 eukaryotic algae and cyanobacteria. *Journal of phycology*. **43**, 605–608 (2007).

110. S. E. Hamsher, K. M. Evans, D. G. Mann, A. Pouličková, G. W. Saunders, Barcoding diatoms: exploring alternatives to COI-5P. *Protist.* **162**, 405–422 (2011).

111. M. Cannon, J. Hester, A. Shalkhauser, E. R. Chan, K. Logue, S. T. Small, D. Serre, In silico assessment of primers for eDNA studies using PrimerTree and application to characterize the biodiversity surrounding the Cuyahoga River. *Scientific reports.* **6**, 22908 (2016).

112. J. G. Caporaso, J. Kuczynski, J. Stombaugh, K. Bittinger, F. D. Bushman, E. K. Costello, N. Fierer, A. G. Pena, J. K. Goodrich, J. I. Gordon, QIIME allows analysis of high-throughput community sequencing data. *Nature methods.* **7**, 335 (2010).

113. R. C. Edgar, UPARSE: highly accurate OTU sequences from microbial amplicon reads. *Nature methods.* **10**, 996 (2013).

114. M. Martin, Cutadapt removes adapter sequences from high-throughput sequencing reads. *EMBnet. journal.* **17**, 10–12 (2011).

115. R. C. Edgar, Search and clustering orders of magnitude faster than BLAST. *Bioinformatics.* **26**, 2460–2461 (2010).

116. C. Camacho, G. Coulouris, V. Avagyan, N. Ma, J. Papadopoulos, K. Bealer, T. L. Madden, BLAST+: architecture and applications. *BMC bioinformatics.* **10**, 421 (2009).

117. R. C. Edgar, H. Flyvbjerg, Error filtering, pair assembly and error correction for next-generation sequencing reads. *Bioinformatics.* **31**, 3476–3482 (2015).

118. R. C. Edgar, UNOISE2: improved error-correction for Illumina 16S and ITS amplicon sequencing. *BioRxiv*, 081257 (2016).

119. P. Yilmaz, L. W. Parfrey, P. Yarza, J. Gerken, E. Pruesse, C. Quast, T. Schweer, J. Peplies, W. Ludwig, F. O. Glöckner, The SILVA and “all-species living tree project (LTP)” taxonomic frameworks. *Nucleic acids research.* **42**, D643–D648 (2013).

120. P.-C. Bürkner, Advanced Bayesian Multilevel Modeling with the R Package brms. *arXiv preprint arXiv:1705.11123* (2017).

121. S. Wasserman, K. Faust, *Social network analysis: Methods and applications* (Cambridge university press, 1994), vol. 8.

122. M. E. Newman, Modularity and community structure in networks. *Proceedings of the national academy of sciences.* **103**, 8577–8582 (2006).

123. S. J. Beckett, Improved community detection in weighted bipartite networks. *Royal Society open science.* **3**, 140536 (2016).

124. T. Hsieh, K. Ma, A. Chao, iNEXT: an R package for rarefaction and extrapolation of species diversity (Hill numbers). *Methods in Ecology and Evolution* (2016).

125. S. J. Brandl, L. Tornabene, C. H. Goatley, J. M. Casey, R. A. Morais, I. M. Côté, C. C. Baldwin, V. Parravicini, N. M. Schiettekatte, D. R. Bellwood, Supplemental Materials for

991 Demographic dynamics of the smallest marine vertebrates fuel coral reef ecosystem
992 functioning. *Science*. **364**, 1189–1192 (2019).

993 126. R. A. Morais, D. R. Bellwood, Global drivers of reef fish growth. *Fish and Fisheries*.

994 127. K. R. Allen, Relation between production and biomass. *Journal of the Fisheries Board of*
995 *Canada*. **28**, 1573–1581 (1971).

996 128. D. Pauly, On the interrelationships between natural mortality, growth parameters, and mean
997 environmental temperature in 175 fish stocks. *ICES Journal of Marine Science*. **39**, 175–
998 192 (1980).

999 129. H. Gislason, N. Daan, J. C. Rice, J. G. Pope, Size, growth, temperature and the natural
1000 mortality of marine fish. *Fish and Fisheries*. **11**, 149–158 (2010).

1001 130. R Core Team, *R: A language and environment for statistical computing*. (2019).

1002 131. H. Wickham, Tidyverse: Easily install and load 'tidyverse' packages. *R package version*. **1**
1003 (2017).

1004 132. J. Oksanen, R. Kindt, P. Legendre, B. O'Hara, M. H. H. Stevens, M. J. Oksanen, M.
1005 Suggests, The vegan package. *Community ecology package*. **10** (2007).

1006 133. G. Csardi, T. Nepusz, The igraph software package for complex network research.
1007 *InterJournal, Complex Systems*. **1695**, 1–9 (2006).

1008 134. C. F. Dormann, B. Gruber, J. Fründ, Introducing the bipartite package: analysing ecological
1009 networks. *interaction*. **1** (2008).

1010 135. M. Kay, tidybayes: Tidy data and geoms for Bayesian models. *R package version*. **1**
1011 (2018).

1012 136. T. Chen, T. He, M. Benesty, V. Khotilovich, Y. Tang, Xgboost: extreme gradient boosting.
1013 *R package version 0.4-2*, 1–4 (2015).

1014 137. R. Lenth, H. Singmann, J. Love, P. Buerkner, M. Herve, Package "emmeans": Estimated
1015 marginal means, aka least-squares means. *Compr. R Arch. Netw*, 1–67 (2019).

1016 138. R. Bauer, Oceanmap: a plotting toolbox for 2D oceanographic data. *R package, version 0.0*.
1017 **9** (2017).

1018 139. D. Pierce, M. D. Pierce, Package 'ncdf4' (2019).

1019 140. R. J. Hijmans, J. van Etten, M. Mattiuzzi, M. Sumner, J. Greenberg, O. Lamigueiro, A.
1020 Bevan, E. Racine, A. Shortridge, Raster package in R (2013).

1021 141. N. M. Schiettekatte, S. J. Brandl, J. M. Casey, *fishualize: Color palettes based on fish*
1022 *species* (CRAN, 2019; <https://CRAN.R-project.org/package=fishualize>).

1023

1024

Acknowledgments

We thank the Environment Agency Abu Dhabi (TMBS/18/L/179) and Dibba Municipality (unnumbered) for collection permits and the UAE Ministry of Environment and Climate Change for the tissue export permit (AUD-Q-22-1110520). All work was performed under NYUAD IACUC approval 18-0003. We further thank the NYU Abu Dhabi Center for Genomics and Systems Biology for sequencing funding and the NYU Abu Dhabi Core Facilities group for support of field collections and thermal experiments. We thank Dain McParland and Grace Vaughan for field support, Noura Al-Mansoori for assistance with processing specimens in the laboratory, and Katherine Maslenikov and Jonathon Huie for assistance in cataloging specimens at the University of Washington. Partial fieldwork funding was provided to L Tornabene by the University of Washington.

Author contributions:

SJB and JLJ designed the study; SJB, JLJ, JMC, and LT performed field collections; JLJ ran physiological trials; SJB, JMC, and LT performed laboratory work; JAB and LT provided funding and resources; SJB performed data analysis and visualization; SJB and RAM performed population modeling; SJB wrote the first draft of the manuscript, and all authors contributed to writing thereafter.

Competing interests:

We declare no competing interests.

Data and materials availability:

All data and code necessary to produce the results are included in this submission and will be made public upon publication of the paper.

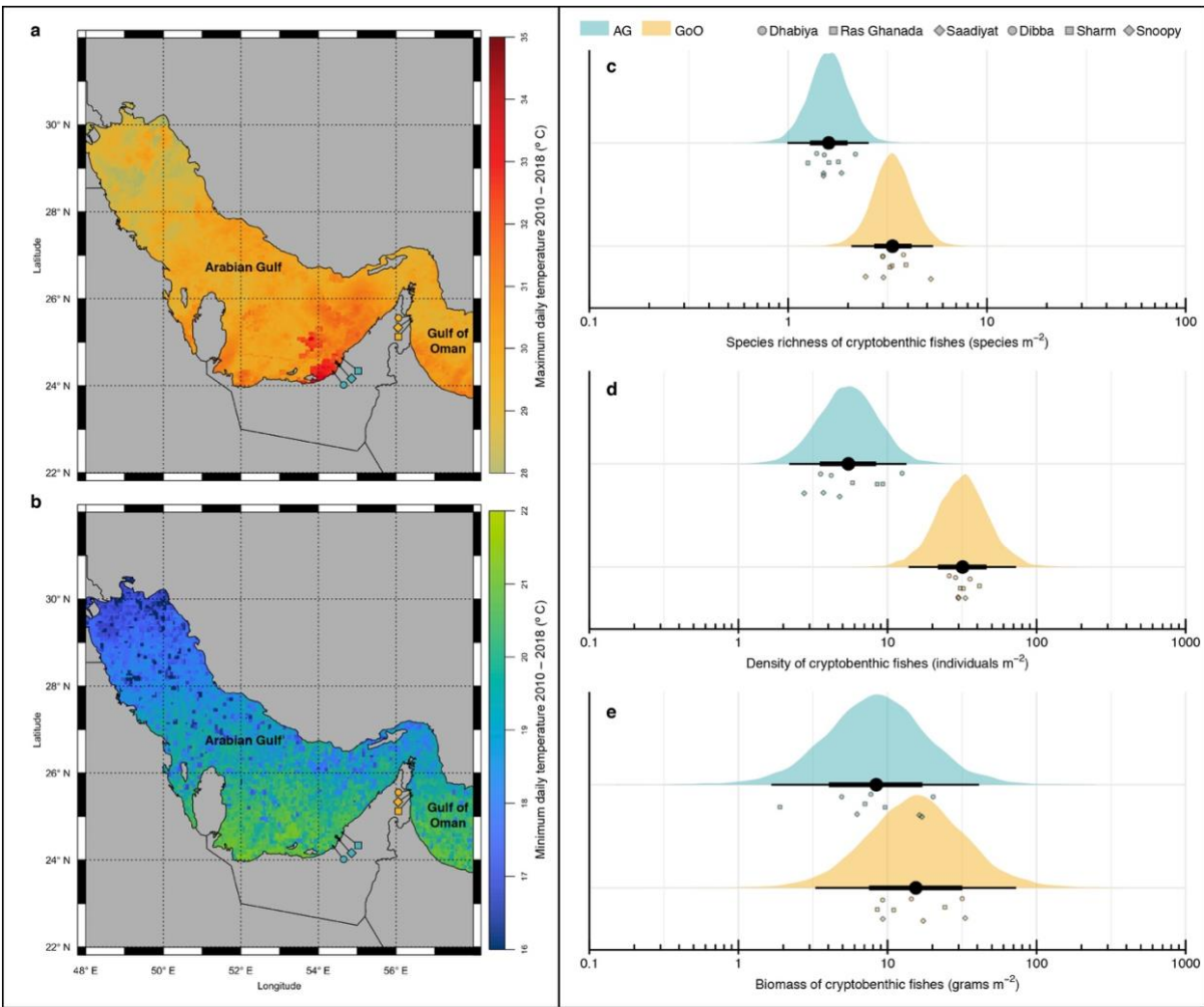


Fig. 1. Map of the study system and community structure of cryptobenthic reef fish communities in the Arabian Gulf (AG) and Gulf of Oman (GoO). (a–b) Maximum and minimum daily temperature estimates for the AG and GoO between 2010 and 2018 (obtained from MODIS Aqua; <https://oceandata.sci.gsfc.nasa.gov/MODIS-Aqua/Mapped/Daily/4km/sst>), with the study sites indicated. (c) Species density and (d) individual density of cryptobenthic reef fishes was markedly higher on reefs in the GoO, while (e) biomass did not substantially differ between the two locations. Density curves represent predicted values based on 1,000 draws from Bayesian hierarchical linear models testing for differences between locations, while black caterpillar plots represent their means, 50%, and 95% credible intervals. Circles, squares, and diamonds represent raw values from the respective sites in each location, jittered on the y-axis.

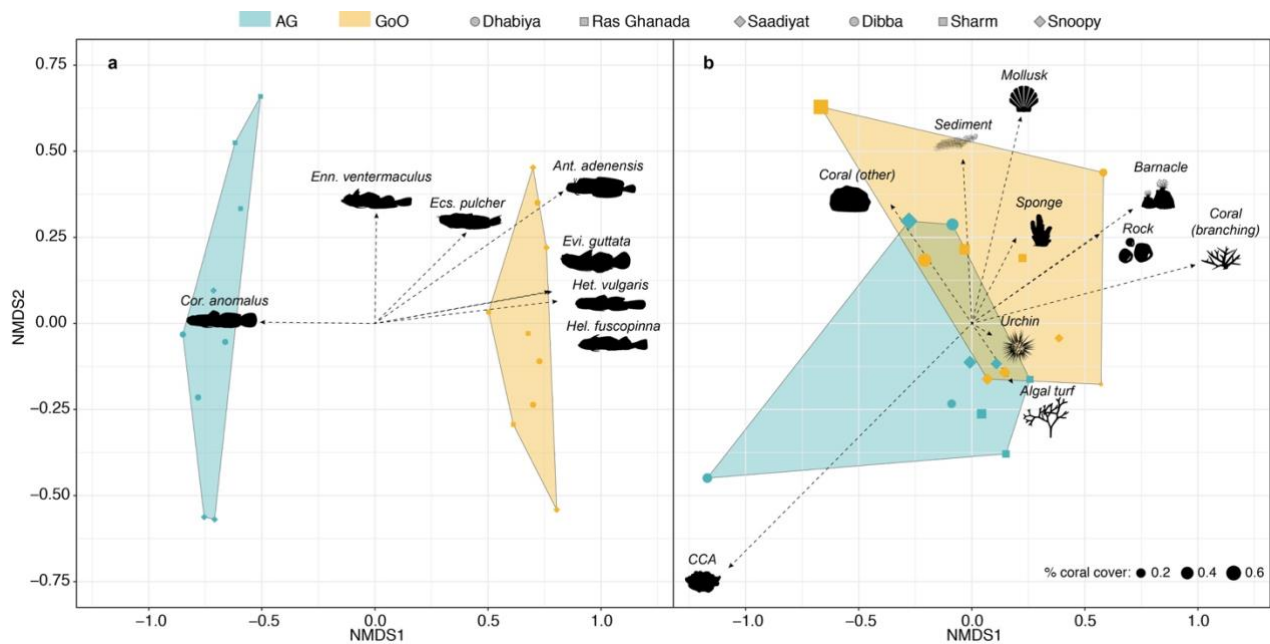


Fig. 2. Community composition of cryptobenthic reef fishes and benthic functional/taxonomic groups in the Arabian Gulf (AG) and Gulf of Oman (GoO). (a) Biplot of a non-metric multidimensional scaling (nMDS) ordination on cryptobenthic fish communities, with the arrows indicating the position and strength of the seven most important species. (b) Biplot of an nMDS on benthic functional groups, with the influence of all groups indicated with arrows. Convex hull polygons delineate the two locations. Each point represents a sample station at a particular site, with the shape size in (b) scaled by percent live coral cover.

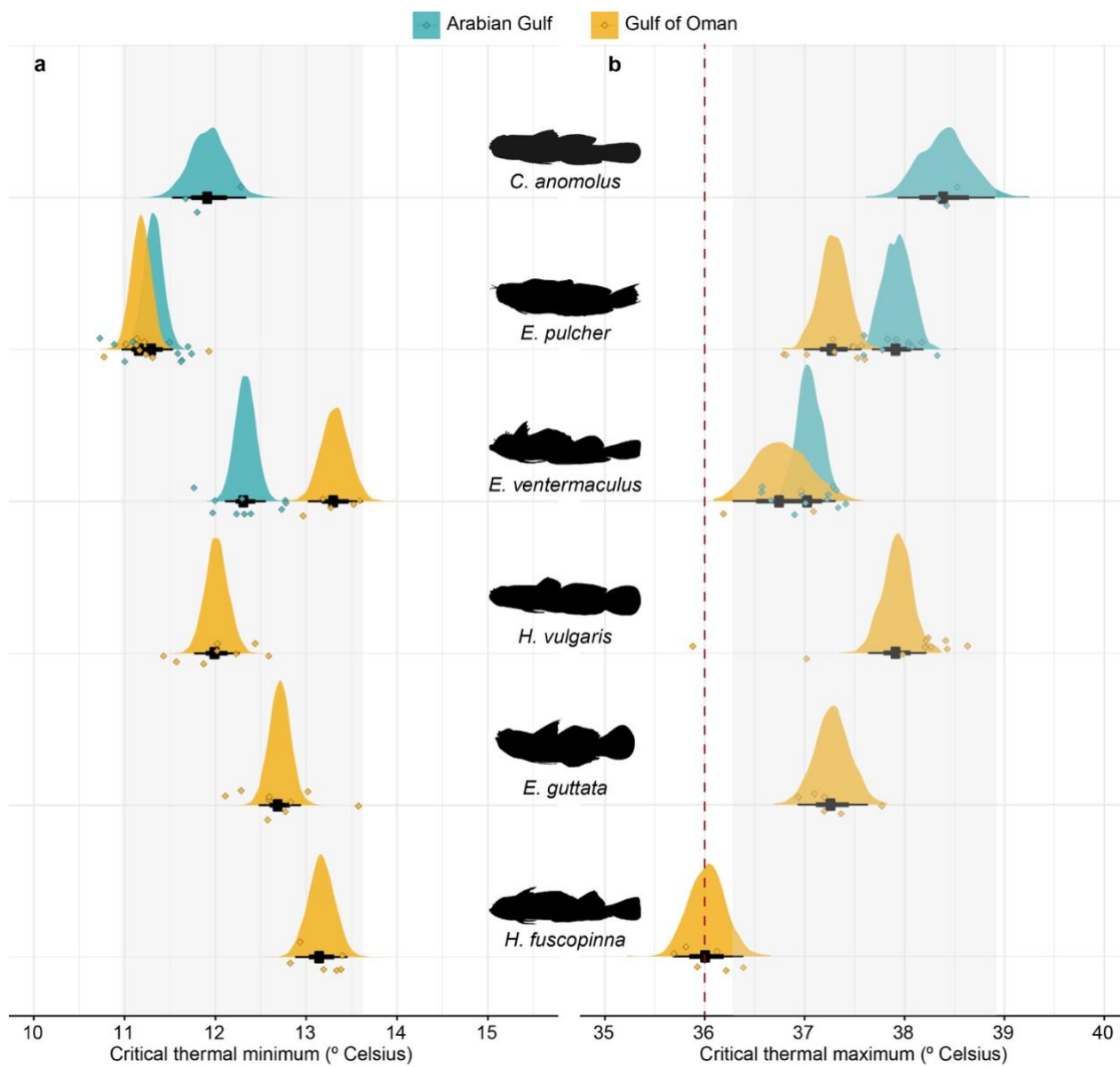


Fig. 3. Critical thermal tolerance limits of cryptobenthic fish species from the Arabian Gulf and Gulf of Oman. (a) Critical thermal minima ranged between 11.9 °C and 13.3 °C, well below the minimum recorded winter temperature for the southern Arabian Gulf (16.0 °C). (b) Critical thermal maxima ranged between 36.0 °C and 38.4 °C, but they were above or equal to the maximum recorded summer temperature in the Arabian Gulf (36.0 °C; red dashed line). Density curves represent fitted values based on 10,000 draws from Bayesian linear models that test for differences among all populations, while black caterpillar plots represent their means, 50%, and 95% credible intervals. Diamonds represent raw values, jittered on the y-axis. Grey boxes delineate the range of the 95% credible intervals obtained for the three species present in the Arabian Gulf.

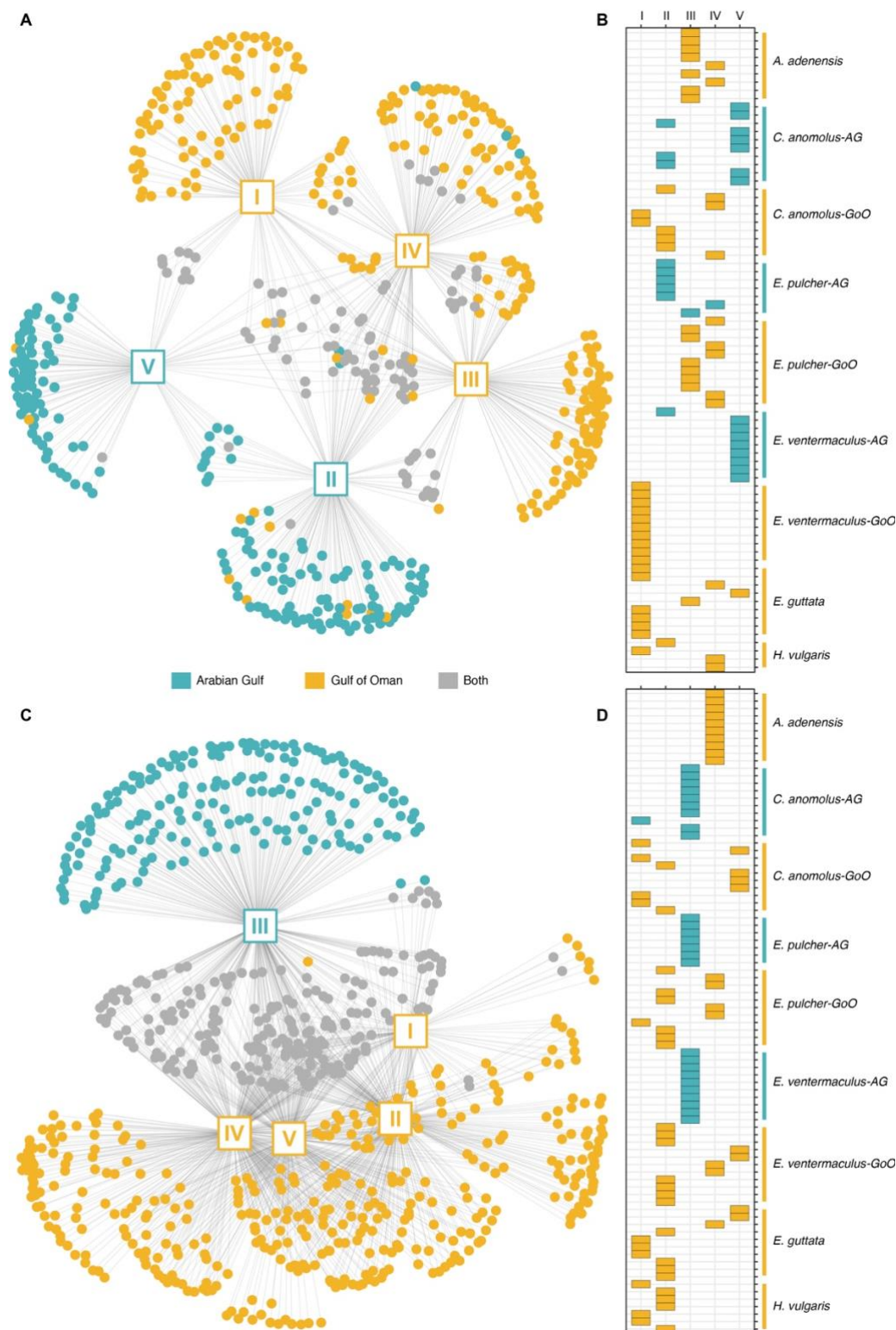


Fig. 4. Diet network trees and modularity mosaics showing differences in ingested prey items and individual-based module membership for COI (a,b) and 23S (c,d) markers. (a,c) Squares with roman numerals represent the recovered modules as nodes in the network tree, while dots represent unique prey items. Blue dots are OTUs (COI) or ESVs (23S) found only in individuals from the Arabian Gulf, gold symbols are from the Gulf of Oman individuals, and grey symbols represent prey items found in individuals from both locations. **(b,d)** Results of the modularity analysis with modules (I-V) as columns and individuals within each species as rows. Colored squares indicate membership in a given module.

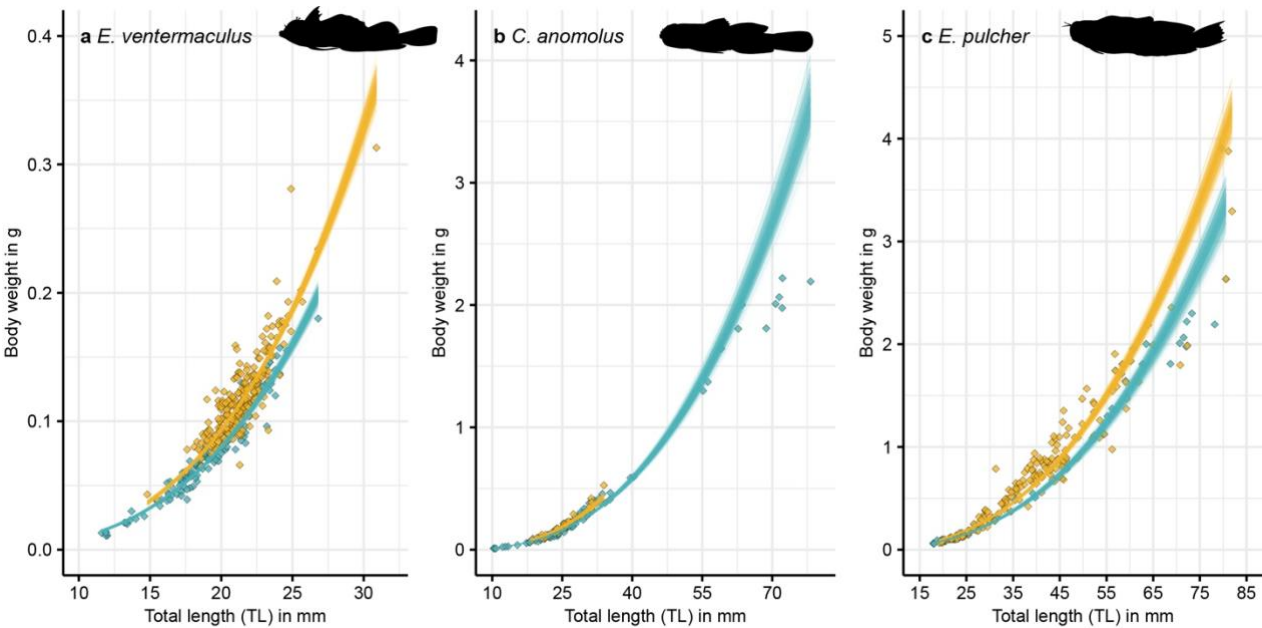
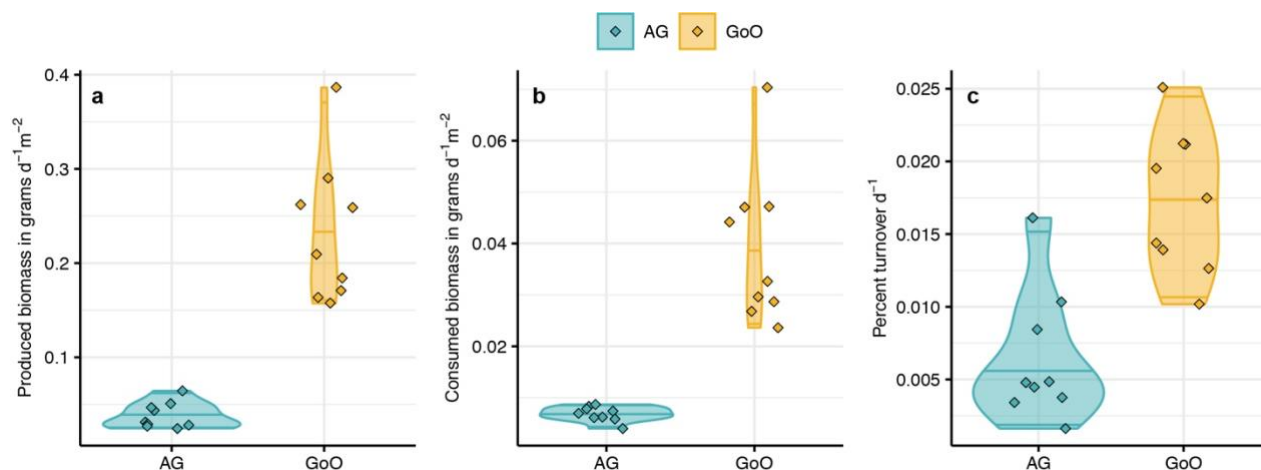


Fig. 5. Relationships between total length (TL) and body weight in populations of *Enneapterygius ventermaculus* (a), *Coryogalops anomolus* (b), and *Ecsenius pulcher* (c) in the Arabian Gulf (blue) and Gulf of Oman (gold). Each line represents a fitted draw from 500 iterations based on the posterior parameters from a Bayesian model regressing length against weight (thus showing model fit uncertainty). Diamonds represent raw values for individual fishes.

1107



1108

1109

1110

1111

1112

1113

1114

1115

1116

1117

1118

Fig. 6. Model estimated biomass production, consumption, and turnover in cryptobenthic fish assemblages across the two locations. (a) Produced biomass (grams of fish tissue grown per day and m^2). **(b)** Consumed biomass (grams of fish tissue perished per day and m^2). **(c)** Percent turnover (renewal of produced and consumed biomass per day). Violin plots and lines represent medians and variance estimates (95% quartiles) for the three metrics across the two locations. Diamonds represent values for each sampled cryptobenthic reef fish community across the six sites (three per site).

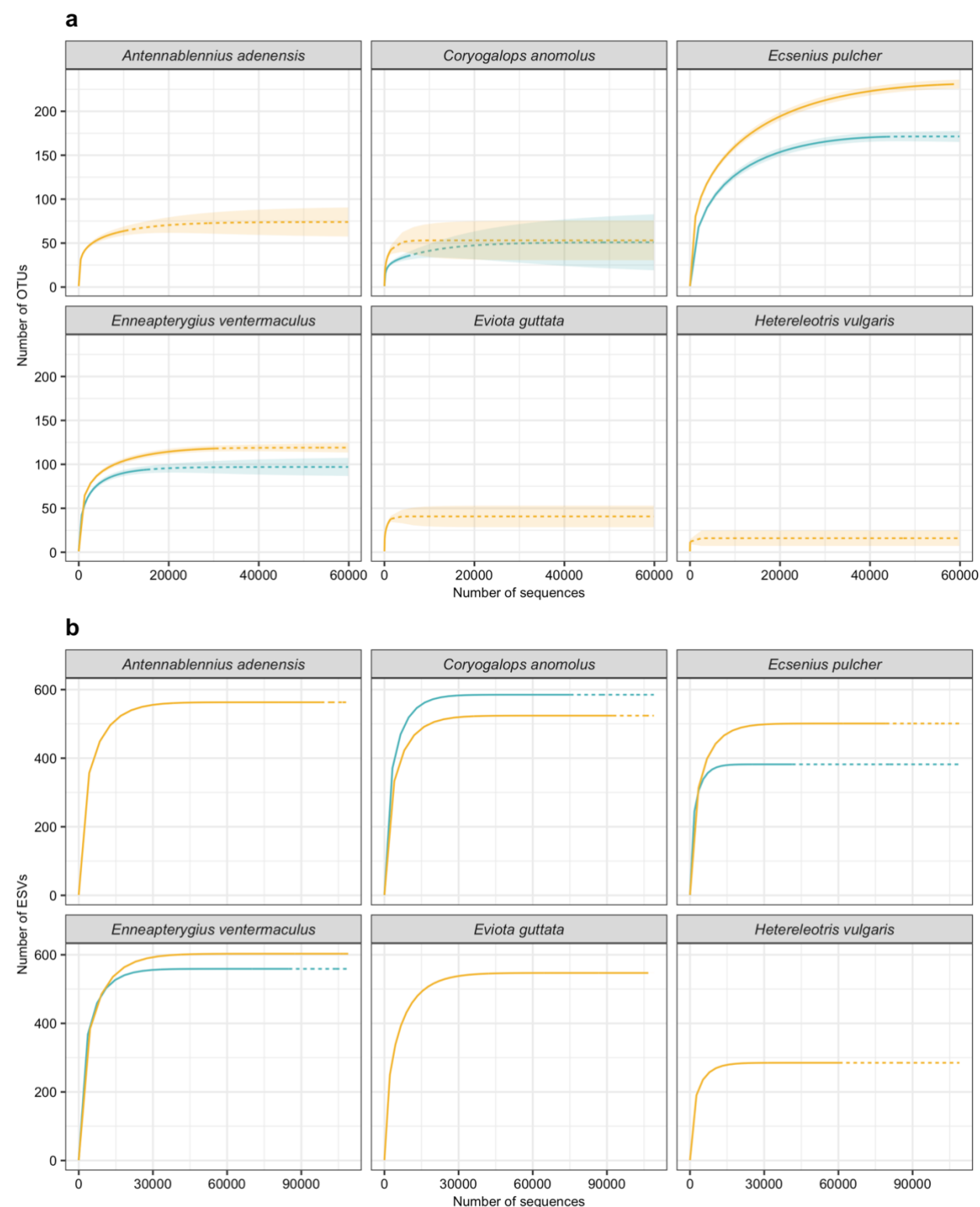


Fig. S1. Rarefaction curves of OTU and ESV richness across total sequences for six species in the Arabian Gulf (blue) and Gulf of Oman (gold). OTU curves (a) indicate the diversity of prey items for each species and population as obtained from gut content DNA metabarcoding with the COI marker, while ESV curves (b) show the diversity of prey items obtained with the 23S marker. Solid lines indicate interpolated richness, while dashed lines indicate extrapolated

richness (to the maximum number of sequences across species). Shaded ribbons indicate 95% confidence intervals of extrapolations.

Table S1. Presence, abundance, and previous records of species sampled in the present study. Each row represents a species, with columns *AG* (Arabian Gulf) and *GO* (Gulf of Oman) indicating the abundance of the species in our samples. Column *R* indicates whether the species has been previously recorded in other parts of the Arabian Gulf (* = yes, – = no). References for previous records are provided.

<i>Family</i>	<i>Species</i>	<i>AG</i>	<i>GO</i>	<i>R</i>	<i>Reference</i>
Apogonidae	<i>Apogon coccineus</i>	6	10	*	present
Apogonidae	<i>Apogonichthyoides taeniatus</i>	2	0	*	present
Apogonidae	<i>Cheilodipterus novemstriatus</i>	2	9	*	present
Apogonidae	<i>Cheilodipterus persicus</i>	0	1	*	Krupp & Müller 1994
Apogonidae	<i>Fowleria variegata</i>	5	1	*	present
Apogonidae	<i>Ostorhinchus cyanosoma</i>	0	15	*	Krupp & Müller 1994
Apogonidae	<i>Ostorhinchus fleuriu</i>	0	30	*	Eagderi et al. 2019
Batrachoididae	<i>Colletteichthys occidentalis</i>	6	0	*	present
Blenniidae	<i>Antennablennius adenensis</i>	0	54	*	Bishop 2003
Blenniidae	<i>Ecsenius pulcher</i>	8	97	*	present
Blenniidae	<i>Laiphognathus multimaculatus</i>	1	0	*	present
Bythitidae	<i>Dinematichthys iluocoeteoides</i>	5	0	*	present
Gobiidae	<i>Asterropteryx semipunctata</i>	0	2	*	Krupp & Müller 1994
Gobiidae	<i>Callogobius bifasciatus</i>	2	0	*	present
Gobiidae	<i>Callogobius speA</i>	0	3	*	Eagderi et al. 2019
Gobiidae	<i>Coryogalops anomalus</i>	65	33	*	present
Gobiidae	<i>Eviota guttata</i>	0	69	*	Krupp & Müller 1994
Gobiidae	<i>Eviota punyit</i>	0	12	*	Krupp & Müller 1994 ₁
Gobiidae	<i>Favonigobius melanobranchus</i>	1	0	*	present
Gobiidae	<i>Fusigobius inframaculatus</i>	0	3	*	Eagderi et al. 2019
Gobiidae	<i>Gnatholepis caudimaculata</i>	0	14	*	Eagderi et al. 2019
Gobiidae	<i>Gobiodon reticulatus</i>	0	2	*	Bishop 2003
Gobiidae	<i>Heteroleotris vulgaris</i>	0	405	*	Eagderi et al. 2019
Gobiidae	<i>Istigobius decoratus</i>	0	15	*	Eagderi et al. 2019
Gobiidae	<i>Priolepis cincta</i>	0	4	*	Winterbottom & Burridge 1992
Gobiidae	<i>Priolepis randalli</i>	0	2	*	Winterbottom & Burridge 1993
Gobiidae	<i>Priolepis semidoliata</i>	0	10	–	NA
Gobiidae	<i>Trimma corallinum</i>	0	11	*	Eagderi et al. 2019 ₂
Muraenidae	<i>Gymnothorax speA</i>	0	12	*	Eagderi et al. 2019 ₃
Ostraciidae	<i>Ostracion cubicus</i>	0	3	*	Eagderi et al. 2019
Pomacanthidae	<i>Pomacanthus maculosus</i>	7	0	*	present
Pomacentridae	<i>Chromis flavaxilla</i>	0	19	*	Bishop 2003
Pomacentridae	<i>Chromis xanthopterygius</i>	0	3	*	Bishop 2003
Pomacentridae	<i>Neopomacentrus cyanomos</i>	0	38	*	Bishop 2003
Pomacentridae	<i>Neopomacentrus miryae</i>	0	38	–	NA
Pomacentridae	<i>Neopomacentrus sindensis</i>	0	6	*	Bishop 2003
Pomacentridae	<i>Pomacentrus aquilus</i>	3	0	*	present
Pomacentridae	<i>Pomacentrus leptus</i>	0	5	*	Bishop 2003
Pomacentridae	<i>Pomacentrus trichrourus</i>	5	0	*	present
Pseudochromidae	<i>Pseudochromis aldabraensis</i>	0	4	*	Bishop 2003
Pseudochromidae	<i>Pseudochromis linda</i>	1	0	*	present
Pseudochromidae	<i>Pseudochromis nigrovittatus</i>	2	1	*	present
Pseudochromidae	<i>Pseudochromis persicus</i>	1	0	*	present
Serranidae	<i>Cephalopholis hemistiktos</i>	2	2	*	present

Syngnathidae	<i>Corythoichthys flavofasciata</i>	0	5	*	Froese & Pauly 2019
Syngnathidae	<i>Doryrhamphus excisus</i>	0	3	*	Bishop 2003
Tripterygiidae	<i>Enneapterygius ventermaculus</i>	131	262	*	present
Tripterygiidae	<i>Helcogramma fuscopinna</i>	0	134	—	NA

identified as *E. sebreei*
synonymous with *T. winterbottomi*
genus level

Table S2. Contrasts between levels of the explanatory variable for the model testing CT_{max} differences in cryptobenthic reef fishes. Population columns highlight the contrast estimated in the model, whereas the estimate and its confidence intervals indicate estimated differences.

Population I	Population II	Estimate	LCI	UCI
<i>C. anomolus</i> .AG	<i>E. pulcher</i> .AG	0.486	-0.079	1.054
<i>C. anomolus</i> .AG	<i>E. ventermaculus</i> .AG	1.360	0.808	1.949
<i>C. anomolus</i> .AG	<i>E. pulcher</i> .GoO	1.114	0.581	1.726
<i>C. anomolus</i> .AG	<i>E. ventermaculus</i> .GoO	1.633	0.939	2.342
<i>C. anomolus</i> .AG	<i>E. guttata</i> .GoO	1.143	0.534	1.759
<i>C. anomolus</i> .AG	<i>H. fuscopinna</i> .GoO	2.392	1.758	2.992
<i>C. anomolus</i> .AG	<i>H. vulgaris</i> .GoO	0.492	-0.061	1.078
<i>E. pulcher</i> .AG	<i>E. ventermaculus</i> .AG	0.879	0.509	1.252
<i>E. pulcher</i> .AG	<i>E. pulcher</i> .GoO	0.636	0.244	1.016
<i>E. pulcher</i> .AG	<i>E. ventermaculus</i> .GoO	1.159	0.624	1.737
<i>E. pulcher</i> .AG	<i>E. guttata</i> .GoO	0.656	0.227	1.134
<i>E. pulcher</i> .AG	<i>H. fuscoguttata</i> .GoO	1.905	1.463	2.341
<i>E. pulcher</i> .AG	<i>H. vulgaris</i> .GoO	0.011	-0.368	0.417
<i>E. ventermaculus</i> .AG	<i>E. pulcher</i> .GoO	-0.245	-0.640	0.118
<i>E. ventermaculus</i> .AG	<i>E. ventermaculus</i> .GoO	0.277	-0.260	0.815
<i>E. ventermaculus</i> .AG	<i>E. guttata</i> .GoO	-0.225	-0.680	0.212
<i>E. ventermaculus</i> .AG	<i>H. fuscopinna</i> .GoO	1.024	0.578	1.449
<i>E. ventermaculus</i> .AG	<i>H. vulgaris</i> .GoO	-0.878	-1.265	-0.508
<i>E. pulcher</i> .GoO	<i>E. ventermaculus</i> .GoO	0.519	-0.0290	1.073
<i>E. pulcher</i> .GoO	<i>E. guttata</i> .GoO	0.020	-0.426	0.494
<i>E. pulcher</i> .GoO	<i>H. fuscopinna</i> .GoO	1.274	0.839	1.726
<i>E. pulcher</i> .GoO	<i>H. vulgaris</i> .GoO	-0.628	-1.037	-0.253
<i>E. ventermaculus</i> .GoO	<i>E. guttata</i> .GoO	-0.502	-1.125	0.106
<i>E. ventermaculus</i> .GoO	<i>H. fuscopinna</i> .GoO	0.750	0.130	1.344
<i>E. ventermaculus</i> .GoO	<i>H. vulgaris</i> .GoO	-1.148	-1.710	-0.584
<i>E. guttata</i> .GoO	<i>H. fuscopinna</i> .GoO	1.252	0.735	1.778
<i>E. guttata</i> .GoO	<i>H. vulgaris</i> .GoO	-0.647	-1.094	-0.148
<i>H. fuscopinna</i> .GoO	<i>H. vulgaris</i> .GoO	-1.906	-2.363	-1.449

Table S3. Contrasts between levels of the explanatory variable for the model testing CT_{min} differences in cryptobenthic reef fishes. Population columns highlight the contrast estimated in the model, whereas the estimate and its confidence intervals indicate estimated differences.

Population I	Population II	Estimate	LCI	UCI
<i>C. anomolus</i> .AG	<i>E. pulcher</i> .AG	0.613	0.173	1.069
<i>C. anomolus</i> .AG	<i>E. ventermaculus</i> .AG	-0.400	-0.851	0.054
<i>C. anomolus</i> .AG	<i>E. pulcher</i> .GoO	0.747	0.316	1.211
<i>C. anomolus</i> .AG	<i>E. ventermaculus</i> .GoO	-1.391	-1.887	-0.888
<i>C. anomolus</i> .AG	<i>E. guttata</i> .GoO	-0.784	-1.241	-0.317
<i>C. anomolus</i> .AG	<i>H. fuscopinna</i> .GoO	-1.235	-1.736	-0.754
<i>C. anomolus</i> .AG	<i>H. vulgaris</i> .GoO	-0.080	-0.549	0.384
<i>E. pulcher</i> .AG	<i>E. ventermaculus</i> .AG	-1.011	-1.313	-0.709
<i>E. pulcher</i> .AG	<i>E. pulcher</i> .GoO	0.137	-0.165	0.446
<i>E. pulcher</i> .AG	<i>E. ventermaculus</i> .GoO	-2.003	-2.402	-1.641
<i>E. pulcher</i> .AG	<i>E. guttata</i> .GoO	-1.394	-1.704	-1.076
<i>E. pulcher</i> .AG	<i>H. fuscopinna</i> .GoO	-1.847	-2.206	-1.489
<i>E. pulcher</i> .AG	<i>H. vulgaris</i> .GoO	-0.694	-1.010	-0.358
<i>E. ventermaculus</i> .AG	<i>E. pulcher</i> .GoO	1.149	0.847	1.459
<i>E. ventermaculus</i> .AG	<i>E. ventermaculus</i> .GoO	-0.990	-1.382	-0.610
<i>E. ventermaculus</i> .AG	<i>E. guttata</i> .GoO	-0.381	-0.706	-0.065
<i>E. ventermaculus</i> .AG	<i>H. fuscopinna</i> .GoO	-0.836	-1.201	-0.475
<i>E. ventermaculus</i> .AG	<i>H. vulgaris</i> .GoO	0.318	-0.016	0.648
<i>E. pulcher</i> .GoO	<i>E. ventermaculus</i> .GoO	-2.138	-2.526	-1.766
<i>E. pulcher</i> .GoO	<i>E. guttata</i> .GoO	-1.530	-1.843	-1.213
<i>E. pulcher</i> .GoO	<i>H. fuscopinna</i> .GoO	-1.985	-2.341	-1.615
<i>E. pulcher</i> .GoO	<i>H. vulgaris</i> .GoO	-0.832	-1.174	-0.519
<i>E. ventermaculus</i> .GoO	<i>E. guttata</i> .GoO	0.607	0.231	1.018
<i>E. ventermaculus</i> .GoO	<i>H. fuscopinna</i> .GoO	0.152	-0.260	0.582
<i>E. ventermaculus</i> .GoO	<i>H. vulgaris</i> .GoO	1.307	0.895	1.691
<i>E. guttata</i> .GoO	<i>H. fuscopinna</i> .GoO	-0.453	-0.822	-0.088
<i>E. guttata</i> .GoO	<i>H. vulgaris</i> .GoO	0.700	0.360	1.041
<i>H. fuscopinna</i> .GoO	<i>H. vulgaris</i> .GoO	1.153	0.799	1.543